

5-2016

Modeling and Parameter Estimation of Escherichia Coli Bioprocess

Ajay Padmakumar

Clemson University, ajaypadmakumar@gmail.com

Follow this and additional works at: https://tigerprints.clemson.edu/all_theses

Recommended Citation

Padmakumar, Ajay, "Modeling and Parameter Estimation of Escherichia Coli Bioprocess" (2016). *All Theses*. 2448.
https://tigerprints.clemson.edu/all_theses/2448

This Thesis is brought to you for free and open access by the Theses at TigerPrints. It has been accepted for inclusion in All Theses by an authorized administrator of TigerPrints. For more information, please contact kokeefe@clemson.edu.

MODELING AND PARAMETER ESTIMATION OF ESCHERICHIA COLI BIOPROCESS

A Thesis
Presented to
the Graduate School of
Clemson University

In Partial Fulfillment
of the Requirements for the Degree
Master of Science
Electrical Engineering

by
Ajay Padmakumar
May 2016

Accepted by:
Dr. Richard Groff, Committee Chair
Dr. William Harrell
Dr. Sarah Harcum

Abstract

Most biopharmaceuticals today are focused on the production of one of three major cell types: the bacterium *Escherichia coli*, yeasts (*Saccharomyces cerevisiae*, *Pichia pastoris*) and mammalian cells (Chinese Hamster Ovary cells). Growth optimization is a major focus as this dictates the pace of advancements in drug manufacturing. The process involved in producing these cells itself is very complex and modeling a system to accurately capture these characteristics can be difficult. The overall process is expensive to run and repeated testing of various control algorithms to optimize growth can prove to be very time consuming as well. In order to develop control strategies and improve the yield of protein, it is beneficial to model a system that captures the responses of the bioprocess. The model can be coupled with different controllers to test the yield output and determine the most effective control strategies without incurring additional costs or time delays. Model parameters are determined by the process of numerical minimization, making use of experimentally obtained data to ensure accurate simulation system behavior. Additionally, a separate system can be developed to switch between the simulation platform and the actual process, with the same control strategy being implemented to compare against results of the simulation and the actual process. This allows for further adjustments to be made to more effectively model the bioprocess. This thesis describes the implementation of the Xu model, found in literature as the simulation counterpart to an experimental

hardware setup. A hardware-in-the-loop simulation is developed with the ability to accurately model system parameters against experimentally obtained results in order to carry out control strategy testing on the simulation side before switching to the experimental hardware side. Accurate parameter estimation is achieved by fitting simulation results to experimentally logged data to ensure the simulation replicates the behavior of the physical system, and is subsequently verified against non-training data.

Dedication

This work is dedicated to my wife, my parents and my brother in appreciation of their support, love and guidance through the years.

Acknowledgments

I would like to sincerely thank my advisor Dr. Richard Groff for his guidance and feedback. I also thank Dr. Timothy Burg and Dr. Sarah Harcum for their advice and assistance. I would also like to add a special thanks to Dr. Rod Harrell. In addition, I would also like to express my gratitude to the other members of this project, Matthew Pepper and Li Wang for their invaluable support. Finally, I want thank Harshawardhan Karve for his insight and help.

Table of Contents

Title Page	i
Abstract	ii
Dedication	iv
Acknowledgments	v
List of Tables	viii
List of Figures	ix
1 Introduction	1
1.1 Background and Motivation	1
1.2 Problem Statement	2
1.3 Literature Review	2
1.4 Outline	3
2 Design and Methods	5
2.1 Bioreactor Model	5
3 Setup	15
3.1 Bioreactor Setup	15
3.2 Simulation Model	20
3.3 Configuring Simulation Models	25
4 Experimental Procedure	28
5 Experimental Results	33
5.1 Numerical Minimization	33
5.2 Fitting Limitations	40
5.3 Result Analysis	41
6 Conclusion and Future Work	46

Appendices	49
A FermSim Model	50
B Experiment Details	54
Bibliography	56

List of Tables

2.1	Xu model variables.	14
3.1	List of sensors and communication protocols used.	20
5.1	Estimation parameter description.	34
5.2	Growth block parameter numerical minimization best fit values. . . .	40
5.3	Error comparison for Fitted vs Xu parameters for the verification experiment.	41
5.4	Objective function weights for each term.	44
1	List of sensors and communication protocols used.	53
2	List of all online and offline variables recorded in database. Experiment number is denoted by i	55

List of Figures

2.1	Representation of glucose and oxygen uptake during Oxidative-Overflow, Oxidative-Metabolite Consumption and Oxidative phases of <i>E. coli</i> metabolism.	8
2.2	Representation of glucose metabolism during aerobic overflow in <i>E. coli</i> .	11
2.3	Representation of acetate metabolism during aerobic overflow in <i>E. coli</i> .	12
3.1	Block diagram of overall setup with added sensors.	16
3.2	Block properties of the OPC read block from the OPC toolbox in Matlab/Simulink.	18
3.3	Block properties of the OPC write block from the OPC toolbox in Matlab/Simulink.	19
3.4	User Interface developed along with FermCtrl for easy read/write access of the OPC server variables.	26
3.5	Representation of the Simulink model FermSim along with the input and output variables.	27
4.1	Experimental setup of the bioreactor and related sensors. 1: Glucose balance; 2: Glucose bottle; 3: Bioreactor vessel; 4: DO probe; 5: Stir motor; 6: pH probe; 7: Base balance; 8: Base bottle; 9: Mass flow controller; 10: DCU pumps (top to bottom - acid, glucose, antifoam, base); 11: Bluesens off-gas sensor; 12: DCU; 13: xPC target. [3] . . .	29
4.2	A plot of DO (percent), Stir speed (rpm), pH, Temperature (degree C) and Mass flow (L/min) versus Time(h).	31
4.3	A plot of O_2 (percent), Glucose balance reading (g), Base balance reading (g), Acetate concentration offline measurement (g/L) and Glucose concentration offline measurement (g/L) versus Time (h).	32
5.1	Training experiment 1 plots for A , S , X and OUR using fitted parameters.	37
5.2	Training experiment 2 plots for A , S , X and OUR using fitted parameters.	38
5.3	Training experiment 3 plots for A , S , X and OUR using fitted parameters.	39
5.4	Verification experiment plots for A , S , X and OUR using fitted parameters.	42

5.5	Verification experiment plots for A , S , X and OUR using Xu parameters.	43
1	Simulink model FermSim with input and output variables.	50
2	FermSim with an example control model.	51
3	The S sub-module block.	52

Chapter 1

Introduction

1.1 Background and Motivation

The primary aim of *E. coli* fermentation processes is to maximize biomass yield, with the assumption that more biomass equals more product [1]. Many factors can affect the growth rate of *E. coli*, including temperature, pH, oxygen uptake rate (OUR), acetate levels and substrate feed rates. Testing control strategies to determine maximum yield profiles can be time consuming and costly. Simulated models offer a means to test such strategies without investing large amounts of time and capital. Modeling and parameter estimation of the *E. coli* metabolic process is very beneficial for implementing and testing control strategies aimed at achieving growth optimization. Developing a complete simulation model that mimics the real-world responses of the system, will significantly decrease time and cost involved in conventional testing. Developing this model to run in parallel to the experimental hardware setup and switching between the hardware and simulation allows easy comparison of performances as well as improved system dynamics characterization.

1.2 Problem Statement

Modeling and parameter estimation of the *E. coli* metabolic process is very beneficial for implementing and testing control strategies aimed at achieving growth optimization. A complete simulation model that mimics the real-world responses of the system, will significantly decrease time and cost involved in conventional testing, but can be difficult to implement as there are a lot of factors that need to be included for the system response to resemble the actual culture response including sensor measurement delays, strain on culture due to inhibitory elements and measurement noise. This thesis describes the implementation of the Xu model [2] along with OUR estimation [3] to model *E. coli* dynamics. Additionally, estimation of metabolic parameters by the means of numerical minimization is also performed. The numerical minimization algorithm makes use of experimentally obtained training data logged from a hardware setup and makes use of non-training data for model verification. In addition, the developed system is interfaced to switch between the simulated model and the hardware platform, achieving a hardware-in-the-loop configuration. The method to obtain experimental data and additionally control hardware settings via simulation is also essential to develop a complete testing and verification setup.

1.3 Literature Review

Accurate modeling of bioprocesses can be very challenging. Biological processes are many orders of magnitude more complex than their corresponding simulations [4, 5]. *E. coli* can be modeled in different ways [6, 7, 8]. Some *E. coli* metabolism models account for a single growth rate throughout the culture's fermentation [7, 9], while others such as [10, 2] treat growth rate as a varying quantity.

Many factors influence the growth of *E. coli*. The complexity of the model increases when additional behaviors are taken into consideration. The oxygen uptake rate (OUR) determines the rate at which oxygen is consumed by the cells to process the glucose that is being fed. If the feed rate is low, it can inhibit growth and cause the *E. coli* to go into a dormant state. In contrast, if the feed rate is high, it can result in the production of acetate as a byproduct. Acetate is detrimental to the production of biomass. The growth of *E. coli* is hindered while the system is in this metabolic phase [11], due to the formation of acetate. Models can also choose to account for other variables such as pH [12]. An accurate pH model requires modeling the buffer interaction with the culture in the bioreactor for the simulation model to resemble the experimental fermentation process. It is important to understand what variables are relevant while deciding model design as it is not feasible to account for all biological factors [13, 14, 15, 16].

Parameter estimation is an important aspect in the development of a simulation model of *E. coli* metabolism [17, 18, 19, 20]. The more closely the simulation data resembles the verification data, the more reliable the output of the simulation during testing conditions. The minimization can be performed by making use of multiple fermentation runs simultaneously to ensure accurate modeling of process dynamics.

1.4 Outline

This thesis describes the simulation of the Xu model combined with sensor and actuator models and the fitting strategy used to identify model parameters of the physical system. This work is divided into the following chapters:

Chapter 2 gives a detailed overview of the model design and model parameters.

E. coli metabolism is explained in detail in this section in order to get better insight into culture behavior. Additionally, the description of the model selected and the reasoning behind the selection are presented along with the extensions made to the model to suit this particular application.

Chapter 3 describes the experimental set up of the *E. coli* fermentation process with a detailed description of the sensors used. The procedure to perform and log data for the entire culture cycle is presented as well. Information about the software used for data logging and subsequent read/write access are also provided here, along with the relevant toolbox packages involved. This chapter also explains the control model FermCtrl, which is used for testing control strategies and switching between the real-world platform and FermSim, which is the model that is used for simulation of culture behavior.

Chapter 4 presents the numerical minimization method implemented along with the FermSim model to determine parameters, based off of experimentally obtained data. It also presents the error observed in the fitted parameters when compared to the experimentally recorded data.

Chapter 5 concludes the thesis with a summary of the obtained results and recommendations for future work.

Chapter 2

Design and Methods

2.1 Bioreactor Model

Modeling of bioprocesses has been a very important part of control and parameterization. For the testing and optimization of control algorithms, it is essential that the *E. coli* fermentation model accurately represents the complex processes occurring during the culture cycle. In this section, the various model alternatives are discussed briefly.

Growth rate is the most important characteristic for a bioprocess model. The two main types of growth rate models are the yield coefficient model and the uptake rate model. One of the most common uptake rate models found in literature is the Monod model [21]. The Monod equation represents a mathematical form of the growth of microorganisms [22]. A typical Monod equation is of the form:

$$\mu = \mu_{max} \frac{S}{K_s + S} \quad (2.1)$$

where μ is the specific growth rate of the microorganism, μ_{max} is the maximum

specific growth rate, S is the substrate concentration and K_s is the saturation term, the value of the substrate concentration when μ is half of μ_{max} .

2.1.1 Yield Coefficient Model

In the yield coefficient model, there is a single μ that represents the growth rate of the culture during the entire course of the bioprocess [9]. This model can only be used to represent one continuous metabolic behavior and is not valid over a large range of growth rates [7]. The equations that represent a typical yield coefficient model are as follows:

$$\begin{aligned}
\frac{dX}{dt} &= \mu X - \frac{F}{V} X \\
\frac{dS}{dt} &= -\mu Y_{S/X} X - \frac{F}{V} (S - S_{in}) \\
\frac{dA}{dt} &= \mu Y_{A/X} X - \frac{F}{V} A \\
\mu(S, A) &= \frac{S}{K_s + S} \frac{K_i}{K_i + A}
\end{aligned} \tag{2.2}$$

where X is the biomass concentration (g/L), F is the flow rate (L/h) and μ is the growth rate. S represents the substrate concentration (g/L). $Y_{S/X}$ represents the yield coefficient of substrate in grams per gram of biomass (g/g) and $Y_{A/X}$ represents the yield coefficient of acetate in grams per gram of biomass (g/g). Acetate concentration is represented by A (g/L) while K_i represents the inhibition of growth rate μ due to acetate concentration A .

2.1.2 Uptake Rate Model

The *E. coli* have three metabolic states based on their uptake of glucose from the solution, qS . In the first metabolic state, the *E. coli* are growing at a rate μ_1 according to qS . As the glucose concentration in the solution increases, so does qS , up to some unknown qS_{O2max} , yielding the growth rate μ_{1max} . When the *E. coli* is in oxidative metabolism they excrete Carbon-dioxide and some other acidic byproducts, such as lactate and formate. If qS exceeds qS_{O2max} , the capacity to process the glucose oxidatively has been exceeded and the excess absorbed glucose is processed anaerobically, known as overflow metabolism. Biomass is formed during overflow metabolism, at a rate μ_2 , albeit much less efficiently. In this case, the culture is growing at rate of $\mu_{1max} + \mu_2$. In overflow metabolism, the main byproduct is acetate, which can inhibit biomass growth and product formation as the concentration rises. If the feed rate is lowered, qS will drop below qS_{O2max} , and the acetate will start to be consumed via acetate consumption metabolism. In acetate consumption metabolism, the acetate is reabsorbed and processed aerobically alongside the glucose; the biomass growth rate associated with this is μ_3 [23]. The overall growth rate of the culture during the metabolite consumption phase is $\mu_1 + \mu_3$.

Figure 2.1 also shows the growth rates during each phase of the *E. coli* metabolism [3]. The concentration of S in the solution and μ can only be obtained using off-line sensors during fermentation.

The primary difference between the uptake rate model and the yield coefficient model is in the way the growth rate, μ is handled. In the former, there is a separate growth rate μ for each metabolic phase in the bioprocess represented by μ_1 the growth rate for the oxidative phase, μ_2 the growth rate during overflow metabolism and μ_3 the growth rate during metabolite consumption. In the latter, there is only a single

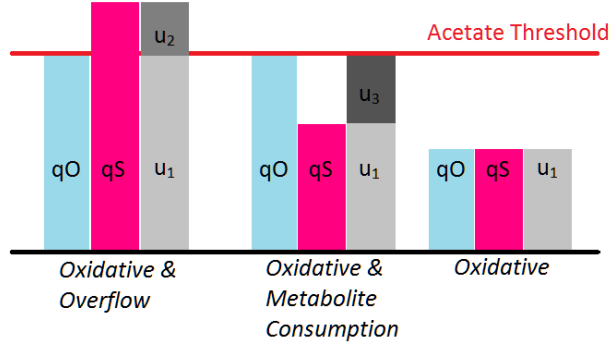


Figure 2.1: Representation of glucose and oxygen uptake during Oxidative-Overflow, Oxidative-Metabolite Consumption and Oxidative phases of *E. coli* metabolism.

growth rate μ throughout the bioprocess.

The acetate has an inhibitory effect on the oxygen uptake rate and results in a smaller growth rate, overall. Therefore, acetate inhibits growth while glucose favors it, but too much glucose results in the system going into overflow and producing more acetate. The advantage of the uptake rate model is that it can take into account, the different metabolic phases and can even rescale the rates of glucose consumption, acetate production or acetate consumption as required. It is more computationally intensive when compared to the yield coefficient model and can only be seen in few of the literature [10, 24, 25]. A typical uptake rate model is represented by the following

set of differential equations:

$$\begin{aligned}
\frac{dX}{dt} &= (\mu_1 + \mu_2 + \mu_3)X - \frac{F}{V}X \\
\frac{dS}{dt} &= (-k_1\mu_1 - k_2\mu_2)X - \frac{F}{V}(S - S_{in}) \\
\frac{dA}{dt} &= (k_3\mu_2 - k_4)X - \frac{F}{V}A \\
\frac{dV}{dt} &= F
\end{aligned} \tag{2.3}$$

where μ_1 , μ_2 and μ_3 represent the growth rates and depend on the uptake which in turn is dependent on the metabolic state of the bioprocess. k_1 , k_2 , k_3 and k_4 represent the yield coefficients.

2.1.3 The Xu Model

The Xu model is an uptake rate model that represents the glucose overflow metabolism in batch and fed-batch cultivation of *E. coli* [2]. The Xu model is selected for this thesis to describe the fermentation process and certain extensions have been made to the model for this study. This model was chosen as it's behavior is closest to the behavior of the *E. coli* observed in the experimental cultures available in the

lab [26]. The mathematical representation of the Xu model is shown below:

$$\begin{aligned}
\frac{dX}{dt} &= \mu X - \frac{F}{V} X \\
\frac{dS}{dt} &= -qSX - \frac{F}{V} (S - S_{in}) \\
\frac{dA}{dt} &= (qA_p - qA_c)X - \frac{F}{V} A \\
\frac{dV}{dt} &= F - F_{sample}
\end{aligned} \tag{2.4}$$

$$\mu = (qS_{ox} - q_m) Y_{X/S_{ox}} + qS_{of} Y_{X/S_{of}} + qA_c Y_{X/A}$$

For the Xu model, biomass concentration X (g/L), glucose concentration S (g/L), acetate concentration A (g/L), volume V (L), oxygen uptake rate OUR (g/L-h) and growth rate μ (1/h) are the state variables and the rate of change of each of these represents the mathematical model. The specific rate of oxygen consumption is represented by qO ($mmol g^{-1} h^{-1}$) and the oxygen uptake rate is obtained as a product of qO and biomass concentration, X . Total glucose uptake is represented by qS while qS_{ox} and qS_{of} are oxidative and overflow fluxes respectively.

In the Xu model, acetate production yields 4 ATP molecules per glucose consumed compared with 2 ATP molecules per glucose for metabolism if anabolic use of glucose is not considered. Taking into consideration the inhibitive effect by acetate on glucose uptake [27, 2], the total glucose uptake rate is given by:

$$qS = \frac{qS_{max}}{1 + A/K_{i,S}} \frac{S}{S + K_S} \tag{2.5}$$

This breaks off into oxidative and overflow fluxes qS_{ox} and qS_{of} and is determined by the boundary condition $qO_S < qO_{max}$. Until this condition is met, all the

glucose is consumed oxidatively and therefore, $qS_{ox} = qS$. Both the oxidative and overflow fluxes are further divided into flux used for anabolism and the remaining used for energy metabolism.

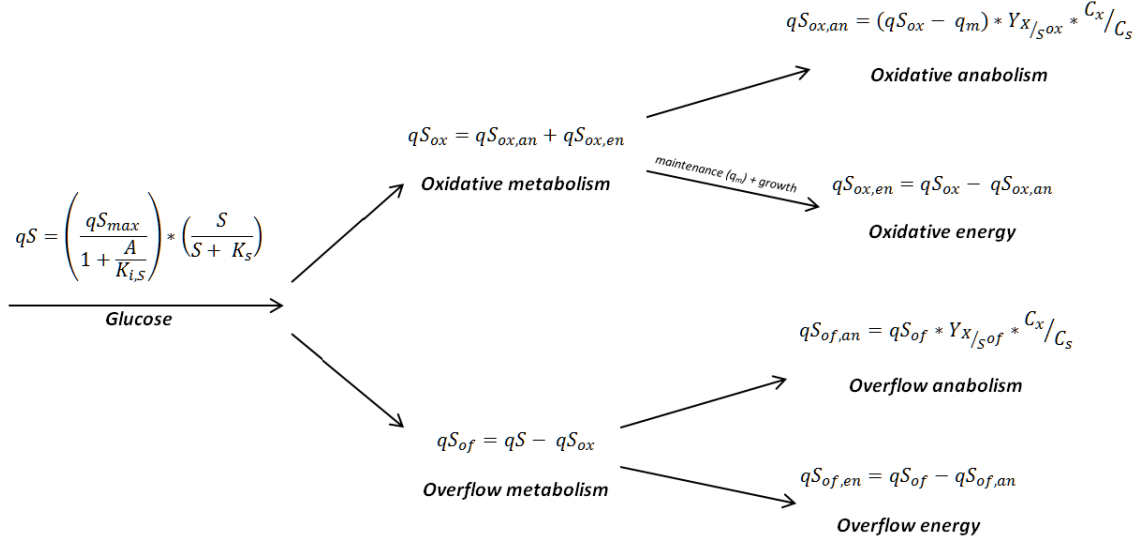


Figure 2.2: Representation of glucose metabolism during aerobic overflow in *E. coli*.

The anabolic flux obtained in oxidative metabolism is a combination of carbon flux used in anabolism, given by $qS_{ox,an}C_S$ and the carbon flux converted to biomass, given by $(qS_{ox} - q_m)Y_{X/S_{ox}}C_X$. Therefore the total glucose flux used in oxidative anabolism is given by:

$$qS_{ox,an} = (qS_{ox} - q_m)Y_{X/S_{ox}} \frac{C_X}{C_S} \quad (2.6)$$

The remaining is used for oxidative aerobic energy metabolism and is given by the expression:

$$qS_{ox,en} = qS_{ox} - qS_{ox,an} \quad (2.7)$$

When the $qO_S = qO_{max}$ the system can no longer process glucose oxidatively and enters overflow. In overflow metabolism, acetate is produced as a byproduct. The rate of glucose used in overflow metabolism is computed from the difference between total glucose uptake qS and total oxidative flux qS_{ox} and is represented as qS_{of} . This is further divided into flux for anabolism and flux for overflow energy metabolism as indicated in Figure 2.2.

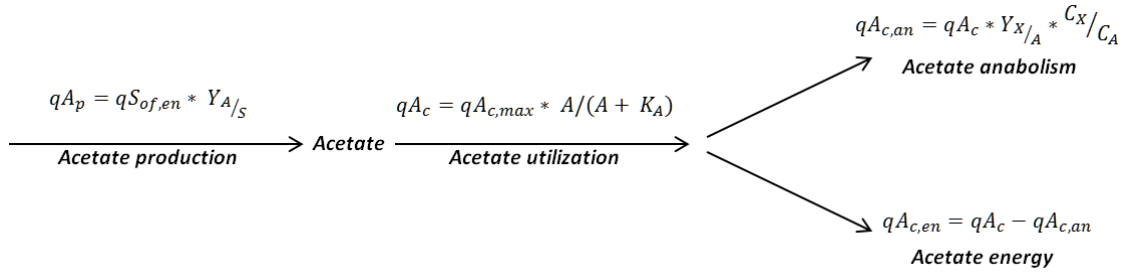


Figure 2.3: Representation of acetate metabolism during aerobic overflow in *E. coli*.

The rate of acetate production is obtained as an expression involving glucose conversion to acetate and the stoichiometric constant $Y_{A/S}$, the yield coefficient of acetate per gram of glucose (g/g):

$$qA_p = qS_{of,en} Y_{A/S} \quad (2.8)$$

While $qO_S < qO_{max}$, the glucose uptake is not saturated and any acetate present in the medium is consumed. The specific rate of acetate consumption is given by the Monod expression:

$$qA_c = qA_{c,max} \frac{A}{A + K_A} \quad (2.9)$$

The consumed acetate is converted to acetyl-CoA, which as discussed earlier, signals the start of the TCA cycle and electron transport chain. The TCA cycle, also

known as the Krebs cycle or the citric acid cycle is a series of enzyme-catalyzed chemical reactions that are an integral part of aerobic respiration in cells. The produced acetate can hypothetically be divided into flux used for anabolism and a "biomass equivalent" flux. These are given by the expressions:

$$\begin{aligned} qA_{c,an} &= qA_c Y_{X/A} \frac{C_X}{C_A} \\ qA_{c,en} &= qA_c - qA_{c,an} \end{aligned} \tag{2.10}$$

The total oxygen consumption rate is a sum of oxygen consumed during the oxidation of glucose and acetate, respectively and is given by the expression:

$$qO = qO_S + qA_{c,en} Y_{O/A} \tag{2.11}$$

A similar combination of growth rates obtained in each of the three metabolic phases- oxidative, overflow and metabolite consumption, gives the total specific growth rate of the system:

$$\mu = (qS_{ox} - q_m) Y_{X/S_{ox}} + qS_{of} Y_{X/S_{of}} + qA_c Y_{X/A} \tag{2.12}$$

These equations are used to model the overall system and the responses can be improved by fitting the parameters involved against experimentally obtained data. This is discussed in further detail in the next chapter.

Symbol (units)	Description	Type
A (g/L)	Acetate concentration	State Variable
S (g/L)	Glucose concentration	State Variable
X (g/L)	Biomass concentration	State Variable
OUR (g/Lhr.)	Oxygen uptake rate	State Variable
qS (g/ghr.)	Glucose flux	Computed (Equation 2.5)
qO (g/ghr.)	Oxygen flux	Computed (Equation 2.11)
qA_p (g/ghr.)	Acetate production flux	Computed (Equation 2.8)
qA_c (g/ghr.)	Acetate consumption flux	Computed (Equation 2.9)
qS_{ox} (g/ghr.)	Glucose oxidative flux	Computed (Equation 2.7)
qS_{of} (g/ghr.)	Glucose overflow flux	Computed (Equation 2.4)
K_A (g/L)	Half rate Acetate Consumption, Monod term	Model Parameter
$K_{i,O}$ (g/L)	OUR inhibition by Acetate	Model Parameter
$K_{i,S}$ (g/L)	GUR inhibition by Acetate	Model Parameter
K_S (g/L)	Half rate Glucose Uptake, Monod term	Model Parameter
$qA_{C_{max}}$ (g/Lhr.)	max Acetate Consumption	Model Parameter
q_m (g/Lhr.)	maintenance	Model Parameter
qO_{max} (g/Lhr.)	max OUR	Model Parameter
qS_{max} (g/Lhr.)	max GUR	Model Parameter
$Y_{A/S}$ (g/g)	g A produced per g S , Stoichiometric const.	Model Parameter
$Y_{O/A}$ (g/g)	g O consumed per g A , Stoichiometric const.	Model Parameter
$Y_{O/S}$ (g/g)	g O consumed per g S , Stoichiometric const.	Model Parameter
$Y_{X/A}$ (g/g)	g X produced per g A	Model Parameter
$Y_{X/S_{of}}$ (g/g)	g X produced per g S , overflow	Model Parameter
$Y_{X/S_{ox}}$ (g/g)	g X produced per g S , oxidative	Model Parameter
F (L/hr.)	Substrate feed rate	Input
V (L)	Culture volume	State Variable

Table 2.1: Xu model variables.

Chapter 3

Setup

This chapter describes the experimental setup of the *E. coli* fermentation. It lists the sensors added to the existing bioreactor setup. A description of the simulation models used to setup hardware-in-the-loop to switch between the simulated fermentation model and the hardware setup, as well as the simulated fermentation model is also provided in this chapter.

3.1 Bioreactor Setup

Industrial and research bioreactor systems are very similar in capability and instrumentation. Bench-top bioreactor systems are used to find appropriate growth profiles, and those growth profiles are scaled up to production capacity. The setup used for this project is representative of these systems. The BioStat B bioreactor system is composed of two hardware components, a double-walled 5 L glass vessel with attached head-plate and a DCU Serial Device controller. A software component, called MFCS/win, runs on a computer. The vessel head-plate contains ports for a pH probe, dissolved oxygen (DO) probe, temperature probe, and motor mount for the

stirrer.

The DCU monitors these probes and implements PID controllers to change water flow for temperature control, add base for pH control and change the stir speed for DO control. The DCU can also feed the culture according to a user-defined feed profile. All commands and sensor data is exchanged with the MFCS/win using the OPC (Object Linking and Embedding (OLE) for Process Control) protocol over RS-422. OPC is a software interface standard that allows Windows to communicate with industrial hardware devices, in this case the DCU. OPC is implemented in server/client pairs where the OPC server converts the hardware communication protocol used by PLCs into OPC protocol. The OPC client uses the OPC server to obtain data from and send commands to the hardware.

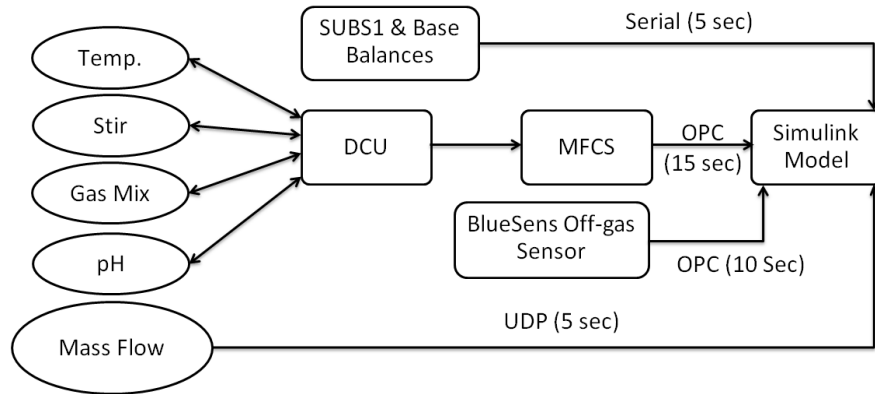


Figure 3.1: Block diagram of overall setup with added sensors.

The MFCS/win logs data from the DCU including motor stir speed, pH levels in the bioreactor tank and substrate base feed rates, and has the capability to perform all controls present on the DCU, as well as combine sensor measurements to form other control variables. Rather than execute just one feed profile, the MFCS/win can also control the fermentation using a serial stack of commands triggered by certain conditions or events. While MFCS/win system is a closed system, it can pass all the

OPC data to an external client, allowing for external control of the system.

Using the OPC toolbox in Matlab/Simulink, it is possible to obtain data from the OPC server and send commands to the hardware via the OPC server. A Simulink model, *FermCtrl* was constructed which could log the fermentation data as well as send commands to the DCU. The model monitors the temperature of the system, stir speed of the shaft, base feed rate, substrate feed rate, pH, and the mix of input gases fed into the bioreactor tank. The OPC Read and OPC Write blocks were used from the Simulink OPC Toolbox library. Both blocks can be implemented in either synchronous or asynchronous modes. If a read operation of an item on an OPC server is synchronous, it reports the last cached reading on the OPC server for that sensor, but an asynchronous read operation reports the current sensor reading. If a write operation on the OPC server is synchronous, the system will pause for confirmation that the value was written, while an asynchronous write does not pause and allows multiple commands to be performed in parallel. The MFCS/win OPC server sends and receives data from the DCU every 15 seconds.

The OPC toolbox allows reading, writing and logging of data from the OPC server to Matlab. It includes Simulink blocks that allow the modeling of online supervisory control and perform hardware-in-the-loop controller testing. Accessing data is done by the means of OPC read and write blocks. They can be configured to run in synchronous or asynchronous mode of operation.

The OPC read block reads data from one or more items on an OPC server. The read operation, as mentioned earlier can take place synchronously from cache or device or asynchronously from device.

The OPC write block writes data to one or more items on an OPC server. The write operation takes place either synchronously or asynchronously.

There were several sensors missing from the system that were found in most

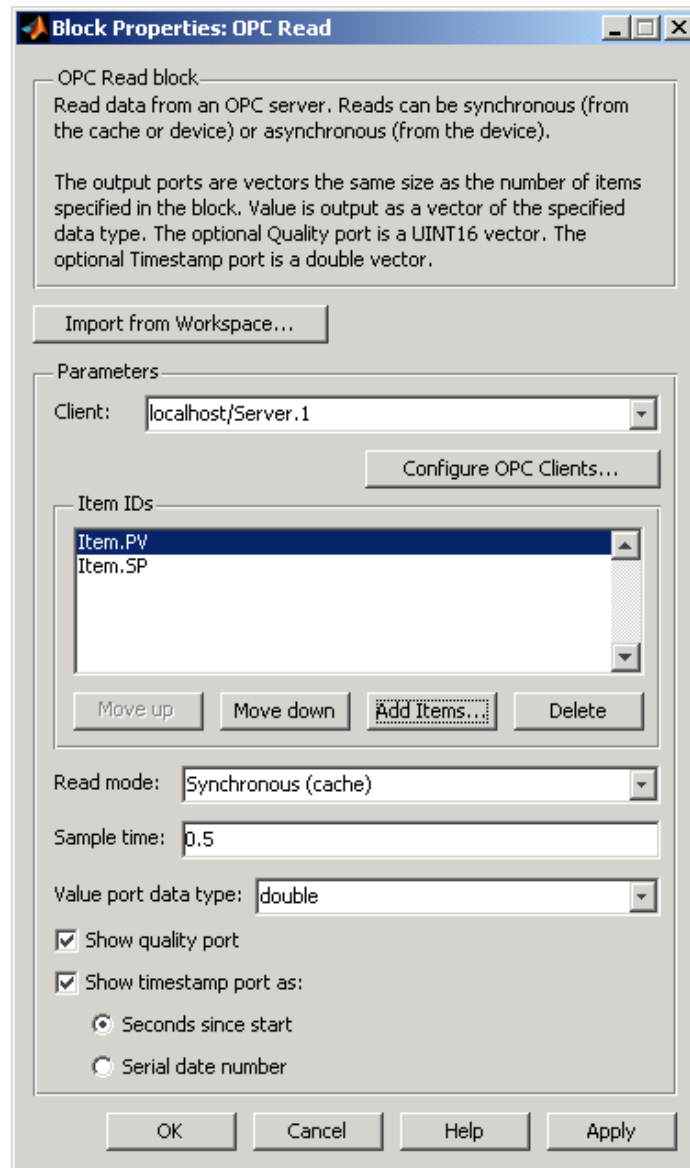


Figure 3.2: Block properties of the OPC read block from the OPC toolbox in Matlab/Simulink.

of the bioprocess control and estimator algorithms papers: a mass flow controller to measure input gas flow rate, balances for exact measurement of the substrate and base feeds, and an off-gas sensor for measurement of exiting oxygen and carbon-dioxide concentrations. These sensors were necessary for implementation of published

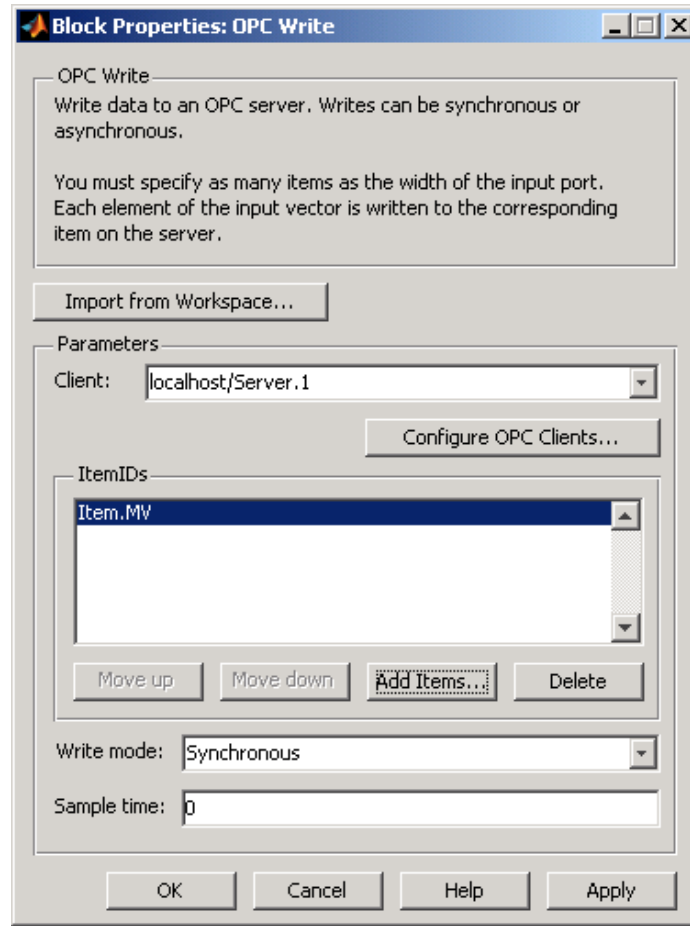


Figure 3.3: Block properties of the OPC write block from the OPC toolbox in Matlab/Simulink.

methods and development of new ones, but the Biostat B DCU was unable to integrate these new signals into the MFCS/win OPC data stream.

The mass flow controller (Omega Engineering Inc., Stamford, CT) was added to control the flow of gas into the bioreactor. The mass flow controller is controlled via an analog voltage input directly mapped to flow rate: $0 - 5V \rightarrow 0 - 10L/min$. An onboard digital display allows confirmation of set mass flow rate. The voltage is supply via a Quanser Q4 board connected to a computer running xPC Target. xPC Target is a Mathworks product that loads in place of the operating system and

executes a compiled Simulink model. In this case, the Simulink model implemented monitors the Ethernet port for commands via user datagram protocol (UDP), which is a networking protocol that doesn't require a handshake to establish a connection or any confirmation from the receiver to transmit a package. A UDP block in the FermCtrl model sets the desired flow rate set-point and receives the flow rate data. The UDP block is set to send/receive data every 5 seconds.

The balances for the substrate and base feed communicate via RS-232 serial every 5 seconds as well. Serial read/write blocks from the Instrument Control Toolbox Simulink library are set to receive the data. The off-gas sensor (BlueSens gas sensor GmbH, Herten, Germany) measures the exhaust gas oxygen and carbon dioxide concentration every 10 seconds. The data is brought in over USB RS-485 and onto a BlueSens OPC server. OPC Read blocks set to asynchronous read receive the data. This can then be used for control purposes.

Sensor	Model	Protocol	Frequency
Mass Flow	Omega Engineering, Stamford, CT	UDP	5 sec
Off-gas	BlueSens Off-gas sensor, Germany	UDP	10 sec
Balance	Ohaus Scout Pro, Newark, JN	Serial	10 sec
DCU	Biostat B, Sartorius, Germany	UDP	15 sec

Table 3.1: List of sensors and communication protocols used.

3.2 Simulation Model

This section describes the two main simulink models developed as a part of this thesis study, namely the FermCtrl model and the FermSim model. The FermCtrl model is the simulink model that makes use of the OPC toolbox to communicate with the OPC servers: MFCS/win that records the sensor data according to settings specified by the DCU and the OPC server that is used to log the Bluesens off-gas

sensor measurement data as shown in Figure 4.1. It is a hardware-in-the-loop implementation with the FermSim simulink model setup in parallel to the OPC read blocks that provide online sensor information from the physical hardware setup, with the ability to switch between the two. The FermSim simulink model contains the Xu uptake rate model described by the ODEs in Equation 2.4. The model also contains an estimator to calculate oxygen uptake rate [3] from the Bluesens O_2 measurements and simulated feed profiles that can be varied to match the experimental feed profiles accurately. In addition, certain other features of these models are discussed in this section in some detail.

3.2.1 FermCtrl Model

The purpose of the FermCtrl model is to implement previously published or new bioprocess control and estimator algorithms. The development of these algorithms was sped up by creating a simulation environment that could mimic the dynamics of the culture, the bioreactor system, and all the sensors. In the first few experiments, the FermCtrl model was used to record data while the MFCS/win and DCU controlled the fermentation. The recorded data is used for sensor and *E. coli* culture characterization. The fundamental sample time of the FermCtrl model is set to 5 seconds and all commands and data are recorded in a .mat file. During later experiments, FermCtrl was used to take control of sensors from the DCU if needed.

The FermCtrl model behaves as a switch between the simulated platform, where the bioprocess is modeled based on mathematical equations and the physical hardware system where data is logged to the OPC server from various on-line sensors. This hardware-in-the-loop approach allows the development and testing of control strategies of high complexity in a fast and accurate manner, with the added benefit

of not straining expensive equipment. Simulation systems offer a way for control to be implemented and tested with regards to efficiency and safety, before porting it to the physical system.

Another advantage of developing such a setup is that numerous tests can be run in a short period of time while conserving material required for actual experimental runs, which also limits waste production.

3.2.2 FermSim Model

The simulation platform, called FermSim, allows testing of control algorithms at a much faster pace when compared to testing it on the physical system. The FermSim parameters are improved by taking experimental results and fitting the simulation parameters to fit the data recorded. By doing this, it is possible to model a simulation as closely as possible to the actual system. The FermSim model developed for this study is an extension of the Xu model, discussed in earlier chapters of this thesis. This section describes the FermSim model used to model culture behavior on simulink.

The FermSim model consists of a growth rate block that contains all the ODEs that make up the Xu model. It has been developed in a way that makes it convenient to change the culture model as required. Another feature of the FermSim model is its initialization file, where all the initial values related to a particular experimental run/strain type can be specified. The model allows custom feed profiles to be input, and can also accept feed profiles directly in the form of a .mat file for both substrate and base feed. This allows reusability while running different characterization experiments and allows the same model to be extended for the parameter fitting using numerical minimization algorithms. In addition, the model has the capacity to accept

both discrete and continuous feed profiles, allowing some flexibility with regards to feed profiles for different control strategies. The stir control block is located outside the bioreactor block, and can be housed with application specific stir control logic. A separate block for OUR estimation is also provided to allow different estimator logics to compute OUR in real time, again based on application needs. The model is developed to run in both hours and seconds and can be switched between one and the other. By designing it in this way, it is possible to use different estimators or control blocks depending on the time step they are configured to. The robustness of this model makes it ideal for estimation and parameter estimation purposes. In Figure 3.5, the separate modules are represented. Each block contains the ODEs required to calculate parameters required for the modeling of the *E. coli* metabolic bioprocess.

3.2.3 OUR Estimator

Sensor dynamics are modeled to obtain a filtered OTR value. This OTR is then used for the computation of OUR. The OUR estimator [3] makes use of qO , which is an output of the growth rate block, to determine OUR of the culture at a given point in time. The volumetric oxygen transfer coefficient k_La can be calculated by the following equation:

$$k_La = a_0 + a_1(N - N_0) \quad (3.1)$$

This equation implies that there is an almost linear relationship between k_La and stir speed N . The constants a_0 , a_1 and N_0 are system/strain specific and are obtained from the initialization files. Subsequently, the k_La is used to calculate the

oxygen transfer rate (OTR).

$$OTR = k_L a (C^* - C) \quad (3.2)$$

Here, C^* is the dissolved oxygen concentration in equilibrium with the gas phase and C is the current dissolved oxygen level. The OUR is calculated by making use of qO the oxygen flux (g/g.h) and the biomass concentration X (g/L).

$$OUR = qOX \quad (3.3)$$

Making use of the OTR obtained in Equation 3.2 and the OUR obtained in Equation 3.3, it is possible to determine the rate of change of C as:

$$\dot{C} = OTR - OUR \quad (3.4)$$

In addition to the OUR calculator, a pH calculator can also be simulated in the FermSim model. This gives information about the pH of the culture and can be used for control if required.

The feed rate can be simulated to discrete pulses based on pump resolutions as well. Based on the type of simulation tests that are being performed, it is possible to input custom fed profiles to the simulated system and obtain corresponding data.

The FermSim model also is used for the fitting of parameters used by the growth rate sub-block in the bioprocess and DCU block to calculate parameters such as growth rate μ , oxygen flux qO , glucose flux qS , acetate consumption flux qA_c and acetate production flux qA_p .

3.3 Configuring Simulation Models

3.3.1 Configuring FermCtrl

FermCtrl makes use of OPC read/write blocks to obtain online data logged in the OPC server and send commands to the DCU during the course of the fermentation. The OPC blocks require the group ID of the reactor it is communicating with, as well as the tags for each of the variables it reads from or writes to. The FermCtrl model can also be used to set the control mode and control status of each of the online sensors with the OPC write blocks. A user interface was created to allow easy access to sensor settings and values as shown in Figure 3.4.

The OPC data read from the server is logged to a destination .mat file. Switching the group ID tags of the OPC read/write blocks to the simulation server allows the FermSim model to run and log data onto the .mat file instead. In this way, FermCtrl acts as a switch between the simulation model and the hardware platform.

3.3.2 Configuring FermSim

For FermSim to run, the .mat file containing the initial values needs to be set up. This initialization file contains all the starting values specific to a fermentation run, including the initial volume in the bioreactor tank, the initial acetate and glucose levels obtained as offline samples and the other constants used in the FermSim model. The full list of initial values is available in the appendix. The type of feed profile being used also needs to be specified. The FermSim model is capable of accepting a purely simulated feed profile or an actual experimental feed profile in the form of a .mat file. The feed can also be discrete pulses or a continuous curve. For the fitting of parameters which is described in greater detail in the next chapters, the actual

The interface is organized into several sections:

- Log File:** A text field for "File Name" and a button labeled "Log File Location".
- Simulation File:** A button labeled "Simulation File".
- Process Variables (pH, Temp, SUBS1, SUBS2, STIRR, DO, Balance):** Each variable has a control panel with:
 - Two "Cont..." dropdown menus.
 - A "Value" display field.
 - A "Set Point" input field.
- O2:** A panel with "Value" (displaying 0) and "Mass Flow" (displaying 0) fields.
- Batch Settings:** A central panel containing:
 - Input fields for "Initial Feed Rate", "Glucose Yield Coeff.", "Initial Volume", and "Glucose Concentration".
 - A "Batch Settings" sub-panel with "Fed Batch Phase Length" and "Batch Phase Length" input fields.
 - An "Offline Sample" button.
- Action Buttons:** "DO Calibration", "Display Graph", and "Start Logging" are located on the right side.

Figure 3.4: User Interface developed along with FermCtrl for easy read/write access of the OPC server variables.

experimental feed profile is used for both glucose and base feeds. There are three inputs to the FermSim simulation model; the stir speed N , the base feed rate F_b and the substrate feed rate F_s . The important output variables of FermSim simulation model are growth rate μ , acetate concentration A , glucose concentration S , biomass concentration X , oxygen uptake rate OUR and base and substrate balance values. All output values are logged to a .mat file for the entire duration of the experiment, along with the simulated culture time.

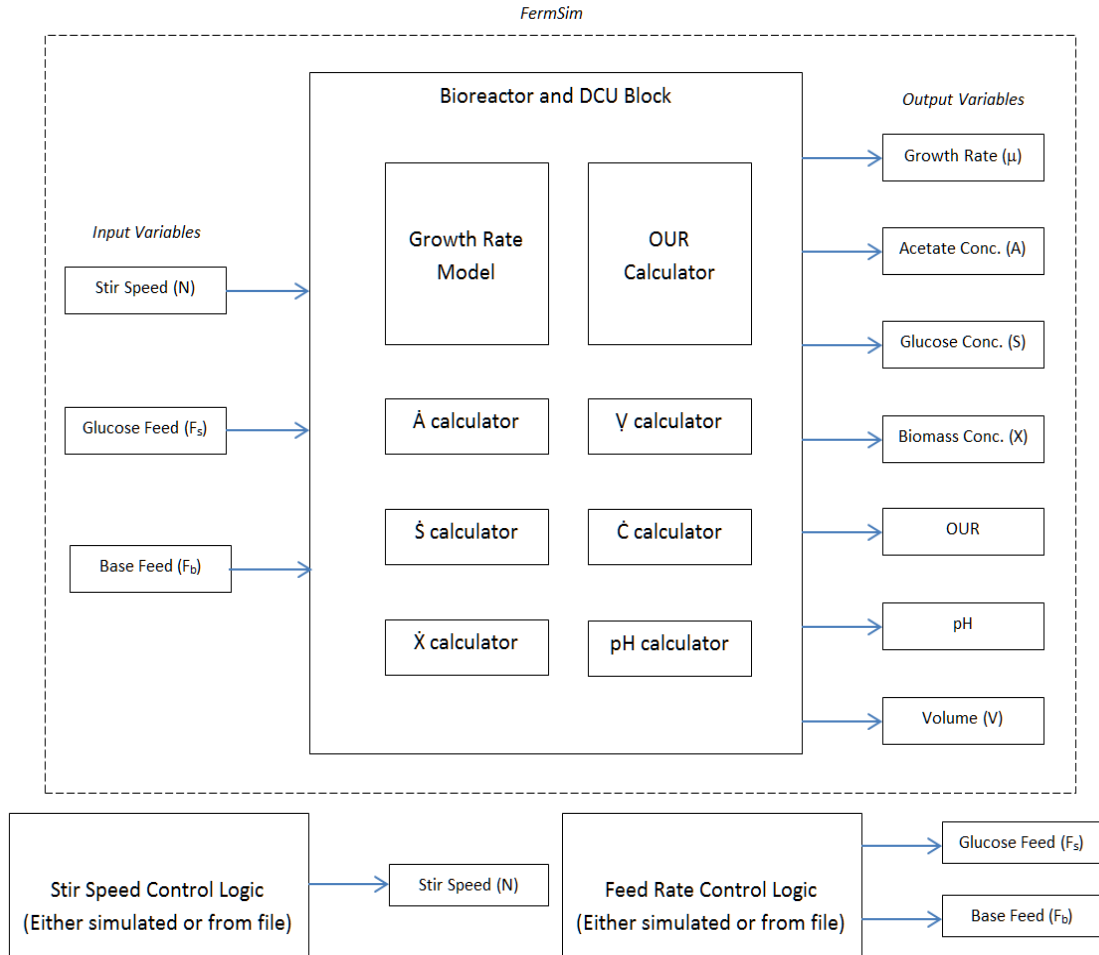


Figure 3.5: Representation of the Simulink model FermSim along with the input and output variables.

The initialization file, called FermSim.mat is experiment specific and is loaded to the simulink workspace before the start of the simulation, for access by FermSim. This allows the same simulation model to be used for all experimental runs, while only requiring the appropriate initialization files and feed profile .mat files.

Chapter 4

Experimental Procedure

This chapter describes the experimental procedure used to perform the *E. coli* fermentation process and log the output data. It also includes information about the offline sampling protocol.

4.0.3 *E. coli* Fermentation Procedure

For the purpose of gathering data of typical *E. coli* fermentation runs, determining sensor delays and system response times, characterization experiments were performed on *E. coli* strain MG1655. This section presents a typical experimental run along with a description of the procedure. Figure 4.1 shows the overall setup of the bioreactor and the related sensors.

The experimental hardware setup is shown in Figure 4.1. The experiment begins with the prepping of the fermenter and positioning of probes and stir blades in the required manner. The sensors are calibrated if needed and primed in the case of the pumps. An overnight culture is introduced into the bioreactor tank after the initial OD measurement is recorded. The feed profile is predetermined and the control is handed to the DCU. The mass flow level is set to the desired level and other

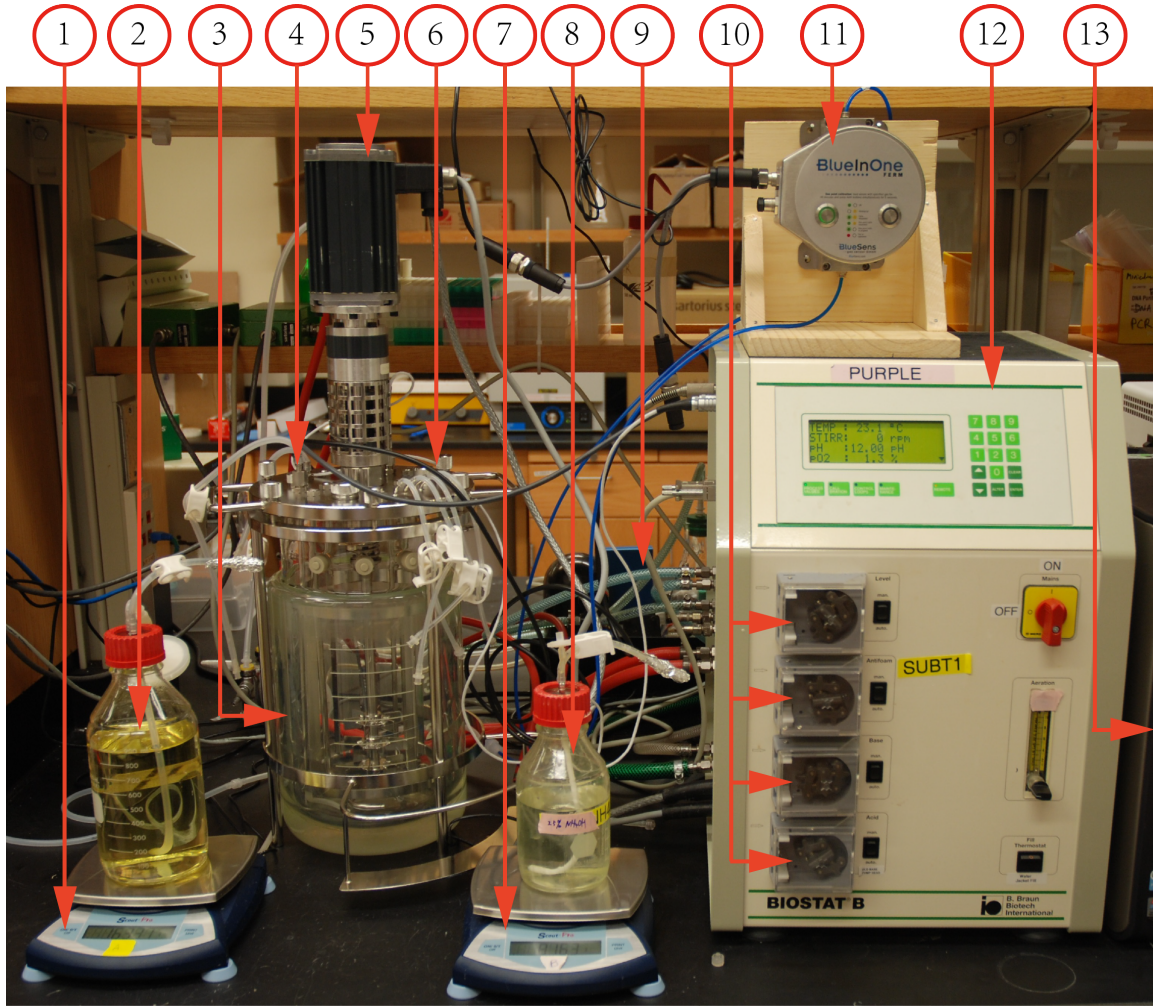


Figure 4.1: Experimental setup of the bioreactor and related sensors. 1: Glucose balance; 2: Glucose bottle; 3: Bioreactor vessel; 4: DO probe; 5: Stir motor; 6: pH probe; 7: Base balance; 8: Base bottle; 9: Mass flow controller; 10: DCU pumps (top to bottom - acid, glucose, antifoam, base); 11: Bluesens off-gas sensor; 12: DCU; 13: xPC target. [3]

additives such as IPTG are introduced into the bioreactor tank when required.

The fermentation process itself consists of two phases, the batch phase and the fed-batch phase. During the batch phase, the cells consume the glucose that is initially present in the bioreactor and rapidly grow. After all the glucose is depleted, the cells start to feed on the acetate, usually indicated by a sudden spike in the dissolved

oxygen level; this marks the end of the batch phase. In fed-batch phase, glucose is fed using an open-loop exponential feed profile or a controlled custom profile. During the fed-batch phase, after the cells reach a predetermined density, chemicals such as isopropyl-beta-thiogalactosidase (IPTG), are added that induce the cells to make the product, usually recombinant proteins [28].

Sampling is done every half an hour and provides the off-line measurements of glucose, OD and acetate levels, which are not obtainable by on-line sensor measurements. During the sampling process, a 1.5 mL sample is taken out of the bioreactor. This sample is used to measure the OD level and then spun down using a centrifuge to remove the bio-material and the remaining liquid is frozen. Once the experiment is complete, the frozen samples are thawed out and used to check for the glucose and acetate levels respective to their sample times. This gives an estimate of the acetate concentration and glucose concentration in the culture during the sampled times. The experiment consists of a batch phase and a fed-batch phase. Typically, the drop in the dissolved oxygen (DO) levels indicates the end of batch phase and the start of fed-batch phase. For the *E. coli* strain used in these experiments, this typically occurs at 5-6 hours culture time.

The plots for on-line measurements and offline measurements of a typical fermentation run with non-induced *E. coli* is shown in Figure 4.3 and Figure 4.2. The glucose concentration and acetate concentration measurements in Figure 4.3 are offline measurements and the rest of the plots are obtained from on-line sensors.

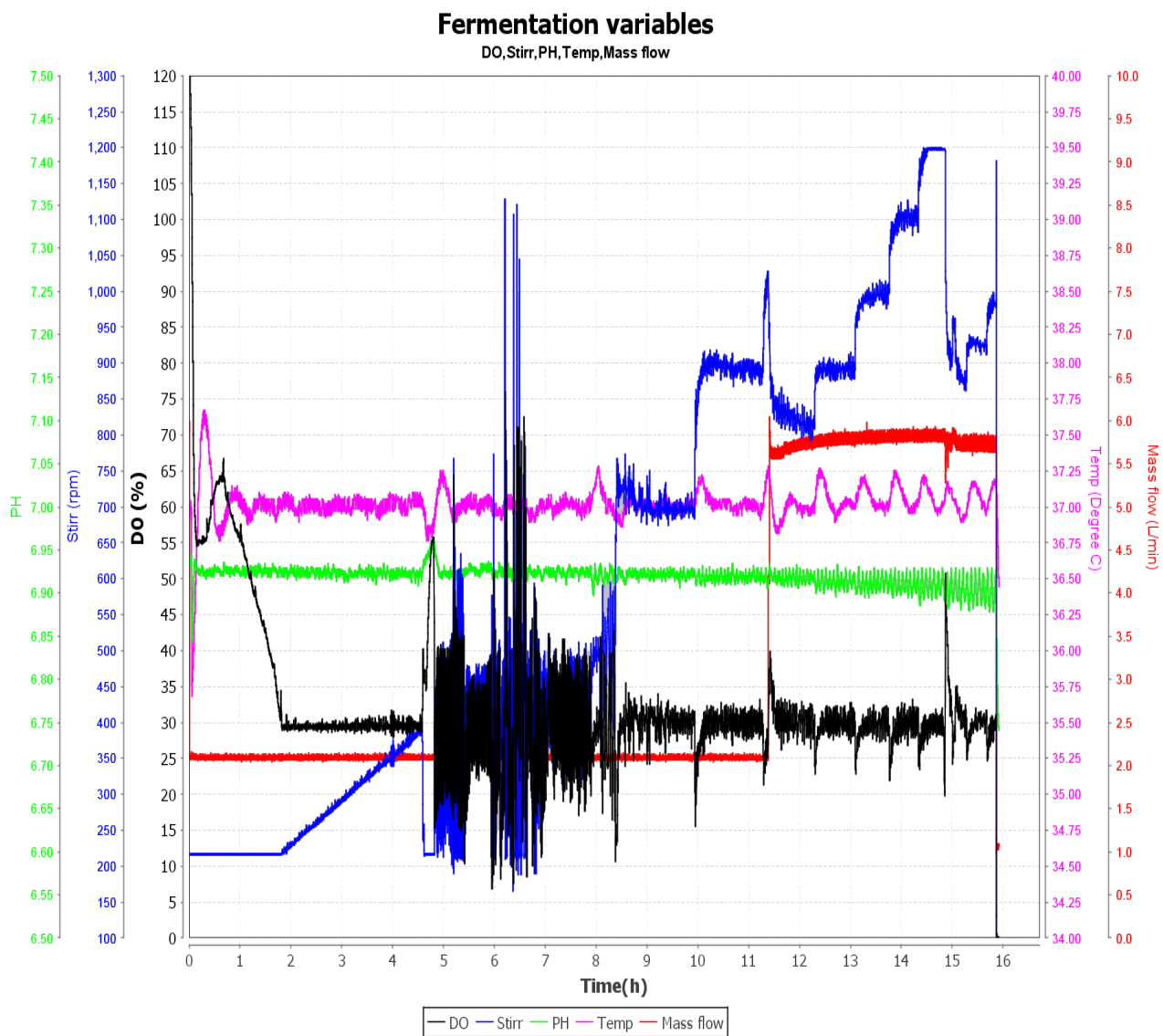


Figure 4.2: A plot of DO (percent), Stir speed (rpm), pH, Temperature (degree C) and Mass flow (L/min) versus Time(h).

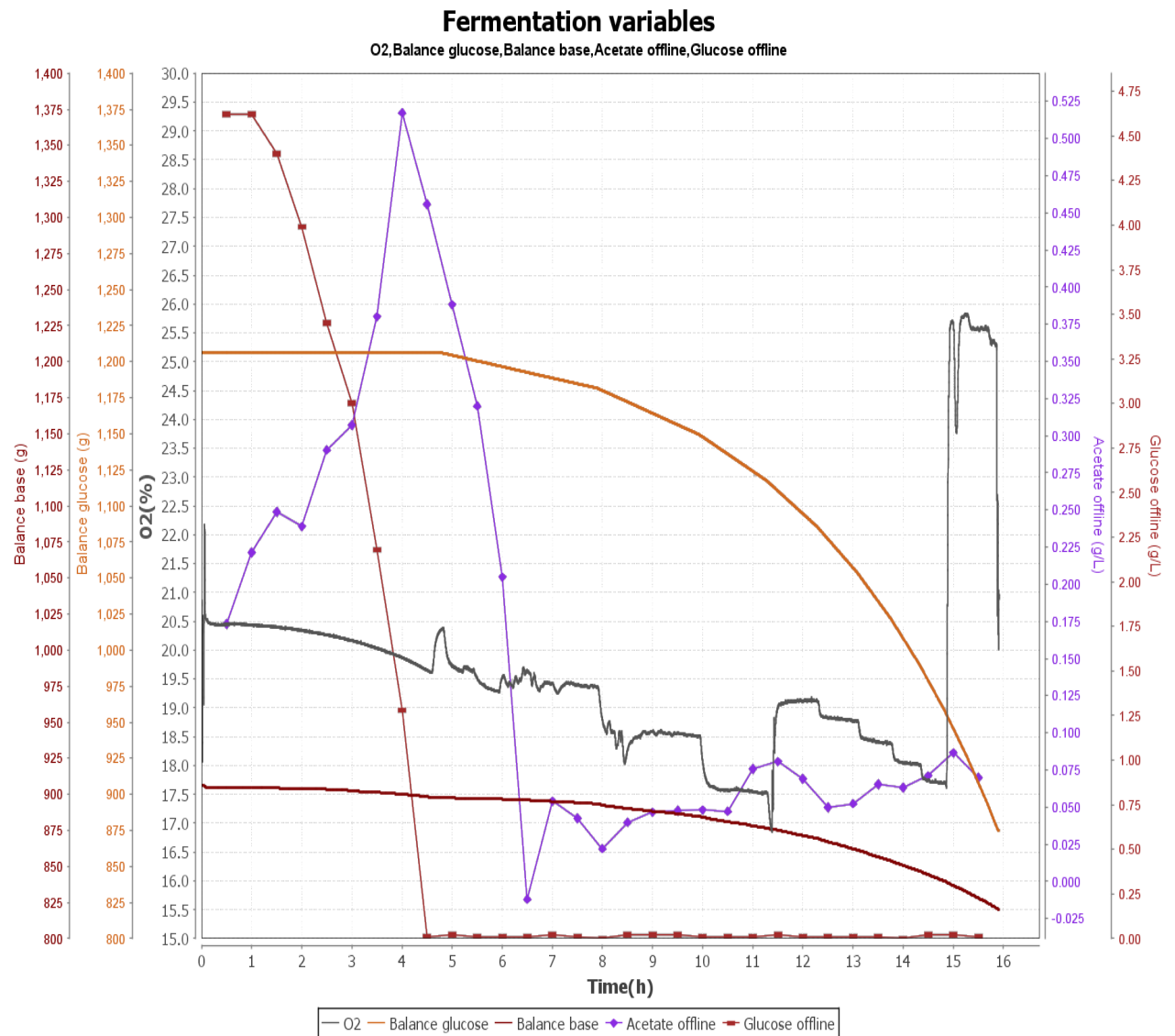


Figure 4.3: A plot of O_2 (percent), Glucose balance reading (g), Base balance reading (g), Acetate concentration offline measurement (g/L) and Glucose concentration offline measurement (g/L) versus Time (h).

Chapter 5

Experimental Results

This chapter presents the results of the parameter estimation algorithm along with the errors observed while fitting using numerical minimization. This chapter also presents the methodology incorporated for parameter estimation by the means of numerical minimization and offers comparison to values used in the original Xu model [2].

5.1 Numerical Minimization

The obtained results are compared to the performance of the original growth block parameters obtained from the Xu model [2].

$$qO_s \leq qO_{max}/(1 + A/K_{i,O}) \quad (5.1)$$

The half rate consumptions for glucose uptake and acetate consumption are Monod terms described in the Equations 2.5 and 2.9. $K_{i,S}$ represents the inhibition term in Equation 2.5 and $K_{i,O}$ is the boundary condition term in Equation 5.1. K_A and K_S are empirical coefficients to the Monod equation, and are *E. coli* strain

Variable (units)	Description
K_A (g/L)	Half rate Acetate Consumption, Monod term
$K_{i,O}$ (g/L)	OUR inhibition by Acetate
$K_{i,S}$ (g/L)	GUR inhibition by Acetate
K_S (g/L)	Half rate Glucose Uptake, Monod term
$qA_{C_{max}}$ (g/Lhr.)	max Acetate Consumption
q_m (g/Lhr.)	maintenance
qO_{max} (g/Lhr.)	max OUR
qS_{max} (g/Lhr.)	max GUR
$Y_{A/S}$ (g/g)	g A produced per g S , Stoichiometric constant
$Y_{O/A}$ (g/g)	g O consumed per g A , Stoichiometric constant
$Y_{O/S}$ (g/g)	g O consumed per g S , Stoichiometric constant
$Y_{X/A}$ (g/g)	g X produced per g A
$Y_{X/S_{of}}$ (g/g)	g X produced per g S , during overflow metabolism
$Y_{X/S_{ox}}$ (g/g)	g X produced per g S , during oxidative metabolism

Table 5.1: Estimation parameter description.

specific. The half rate acetate consumption is set to 0.05 and the half rate glucose consumption is set to 0.05 [2].

$Y_{A/S}$, $Y_{O/A}$ and $Y_{O/S}$ are stoichiometric constants [2]. $K_{i,O}$, $K_{i,S}$, $qA_{C_{max}}$, q_m , qO_{max} , qS_{max} , $Y_{X/A}$, $Y_{X/S_{of}}$ and $Y_{X/S_{ox}}$ are the fitted to three training experiment datasets obtained by the procedure described in Chapter 4.0.3, for three separate feed profiles and initialization files. They are verified against a fourth experimentally obtained dataset that is not used for training. The constraints and stopping conditions of the numerical minimization method determines the accuracy of the fitted parameters.

5.1.1 Minimization Procedure

For the process of parameter estimation of the fermentation model, experimentally obtained datasets from three different experiments are used as training data sets. The data is fed into a Simulink script that runs the FermSim model iteratively,

in an attempt to form a Gaussian and determine the best fit for the selected parameters, based on tolerance conditions and iteration limits. Constrained minimization is performed and the algorithm makes use of an objective function to determine the error between the simulated data and the experimentally recorded data. The Simulink function used for this is `fmincon`. Constraints are set on the upper and lower bounds of the parameter values. The bounds ensure that the minimization does not try to fit to impossible parameter values like values less than zero. The algorithm is not constrained with regards to number of iterations or maximum function evaluations. Tolerances are set for the parameter values, represented as unknowns x and the minimization or objective function error, $fval$.

The feed profiles for substrate and base are obtained directly from the experiment runs. This is provided to FermSim in the form of .mat files. The OUR estimation is also performed in FermSim [3] and the objective function is a weighted function comparing the simulated values of the acetate curve, the glucose curve, the biomass curve and the OUR values against the experimental values at logged values of data. The errors are weighted for each objective function term to ensure that of the offline data measurements is equally important, thereby ensuring that the parameters are fitted accurately.

$$fval = \sum_{i=0}^N [(A_{error}(t_i))^2 + (S_{error}(t_i))^2 + (X_{error}(t_i))^2] + \sum_{j=0}^M (OUR_{error}(t_j))^2 \quad (5.2)$$

where the individual errors are computed as the difference between the simulated and experimental values at time t and N and M are the number of sample points for the offline and online data respectively, for each of the fitting experiments.

Each training dataset produces a $fval$ and the sum of these $fval$ forms the overall objective function's $Fval$. This ensures that a best fit across all training experiments is obtained, as total $fval$ is a sum of individual $Fvals$. Figure 5.1, Figure 5.2 and Figure 5.3 are the three training dataset plots and Figure 5.4 is the verification plot. Each point represents a recorded data point. In the case of acetate concentration A , substrate concentration S and biomass concentration X , these are offline sampled data. In the case of OUR, it is the data logged by the BlueSens in its OPC server.

Each experiment has its own initialization file, feed profile and sampling frequency. In the case of the first training experiment, offline samples were recorded every hour, whereas in the case of the other two training experiments and the verification experiment, offline samples were recorded every half an hour. The developed procedure allows for this sort of staging. The appropriate initial conditions file, feed profiles and sampling information are used by the respective experiment numbers. Using the experimental conditions and feed in the simulation ensures near identical conditions for the simulated environment. Each of the files are read directly from Matlab's workspace during the iterative minimization process and need to be loaded and cleared in succession for each iteration. Any number of training datasets can be added as the setup is very scalable. The initial guess for this minimization was varied and the final result obtained is verified to be a true minimum, for the given constraints. The reason the process is performed multiple times with different initial guesses is to ensure the minimization is returning a true global minimum, and not a local minimum.

The error associated with each term in the overall $Fval$ function determines the degree of fitting to each individual experiment. Further, each of these $fval$ terms consist of the error values due to A , S , X , and OUR. Each of these error values in the $fval$ expression are weighed differently, according to the error magnitude observer. To

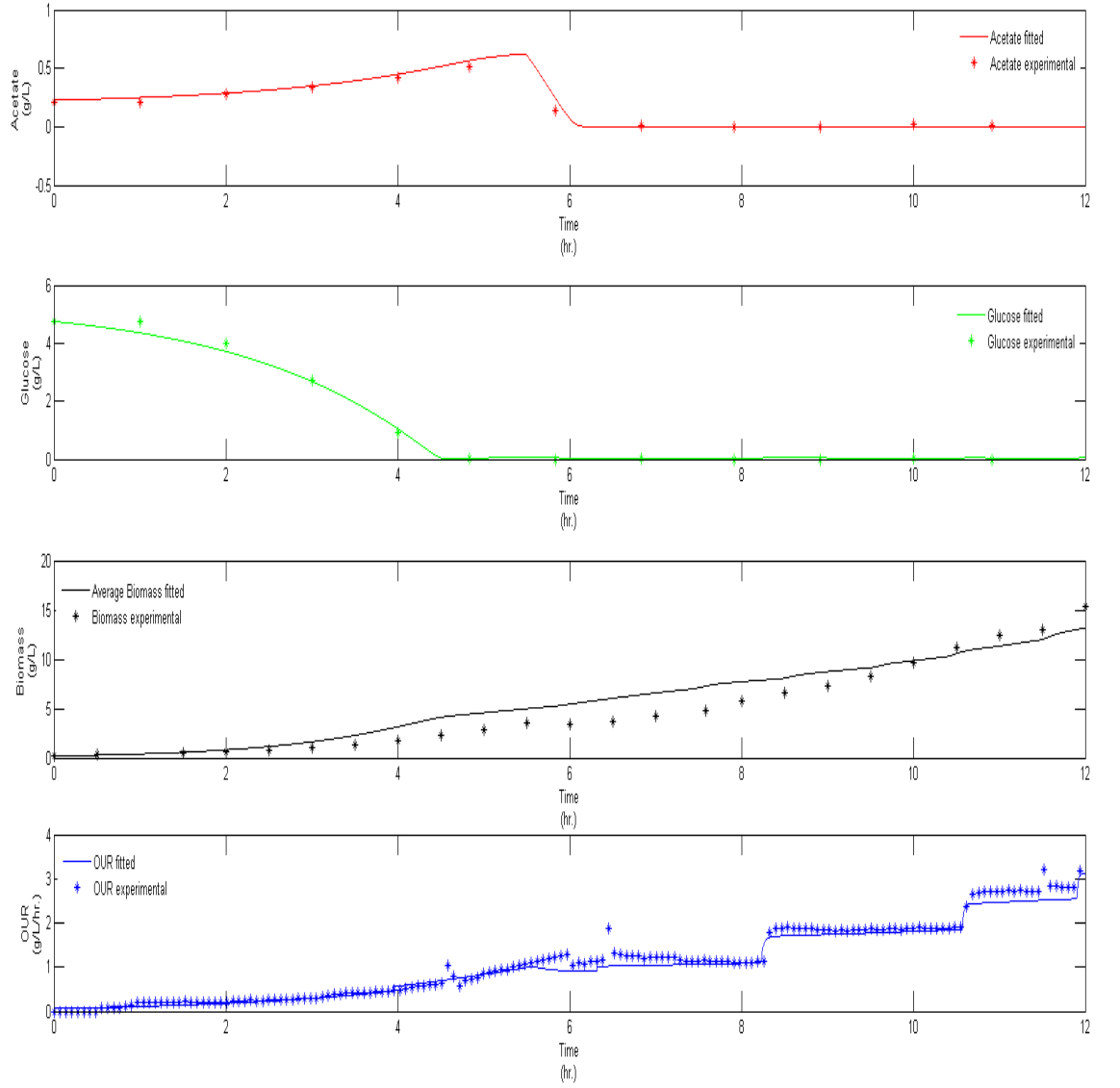


Figure 5.1: Training experiment 1 plots for A , S , X and OUR using fitted parameters.

compare the fitting results with the original Xu parameter values [2], the maximum error associated for each of the objective function curves (A , S , X and OUR) is observed. Table 5.2 shows the minimization result value and the Xu value for each

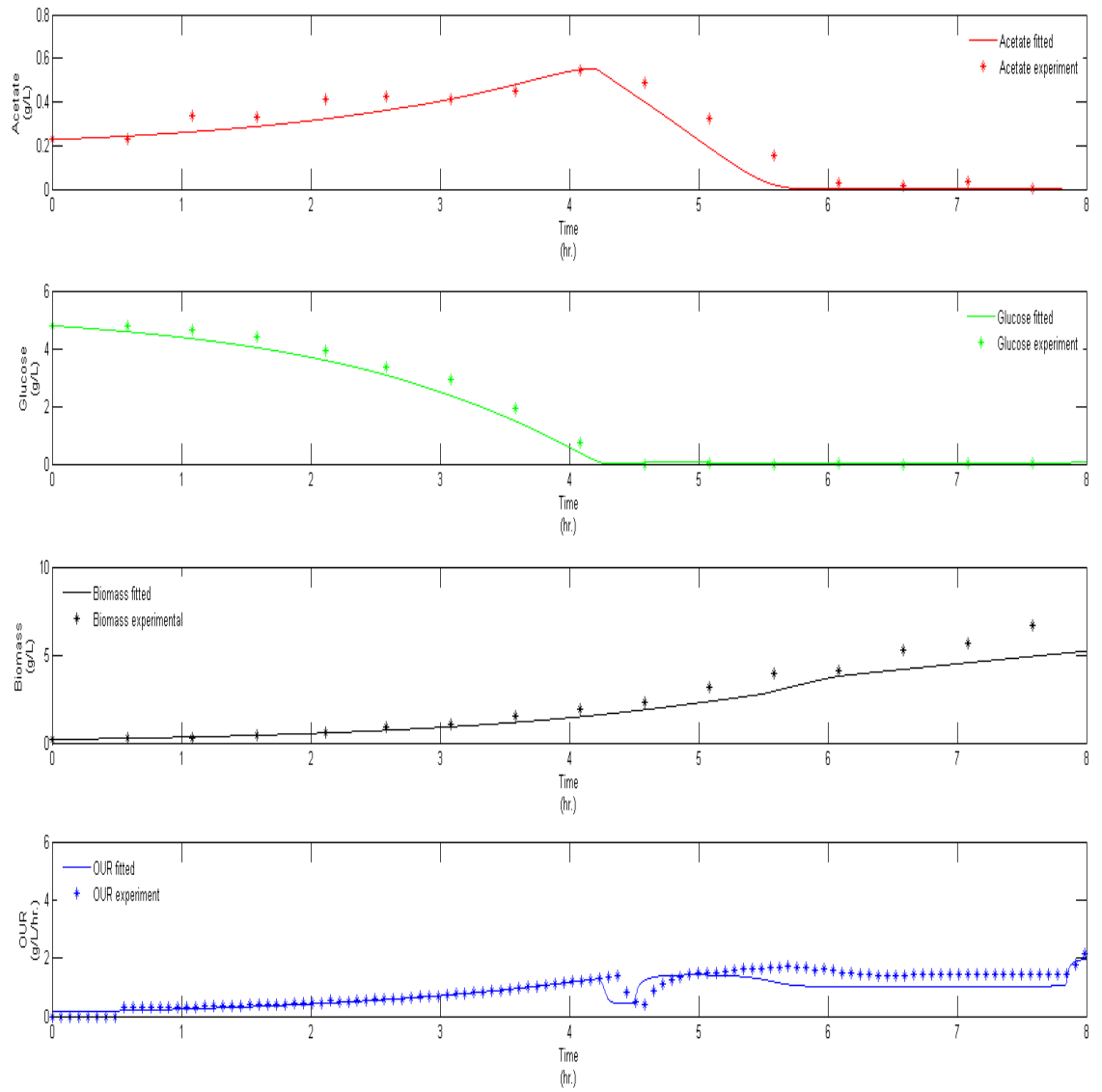


Figure 5.2: Training experiment 2 plots for A , S , X and OUR using fitted parameters.

of the fitted parameters.

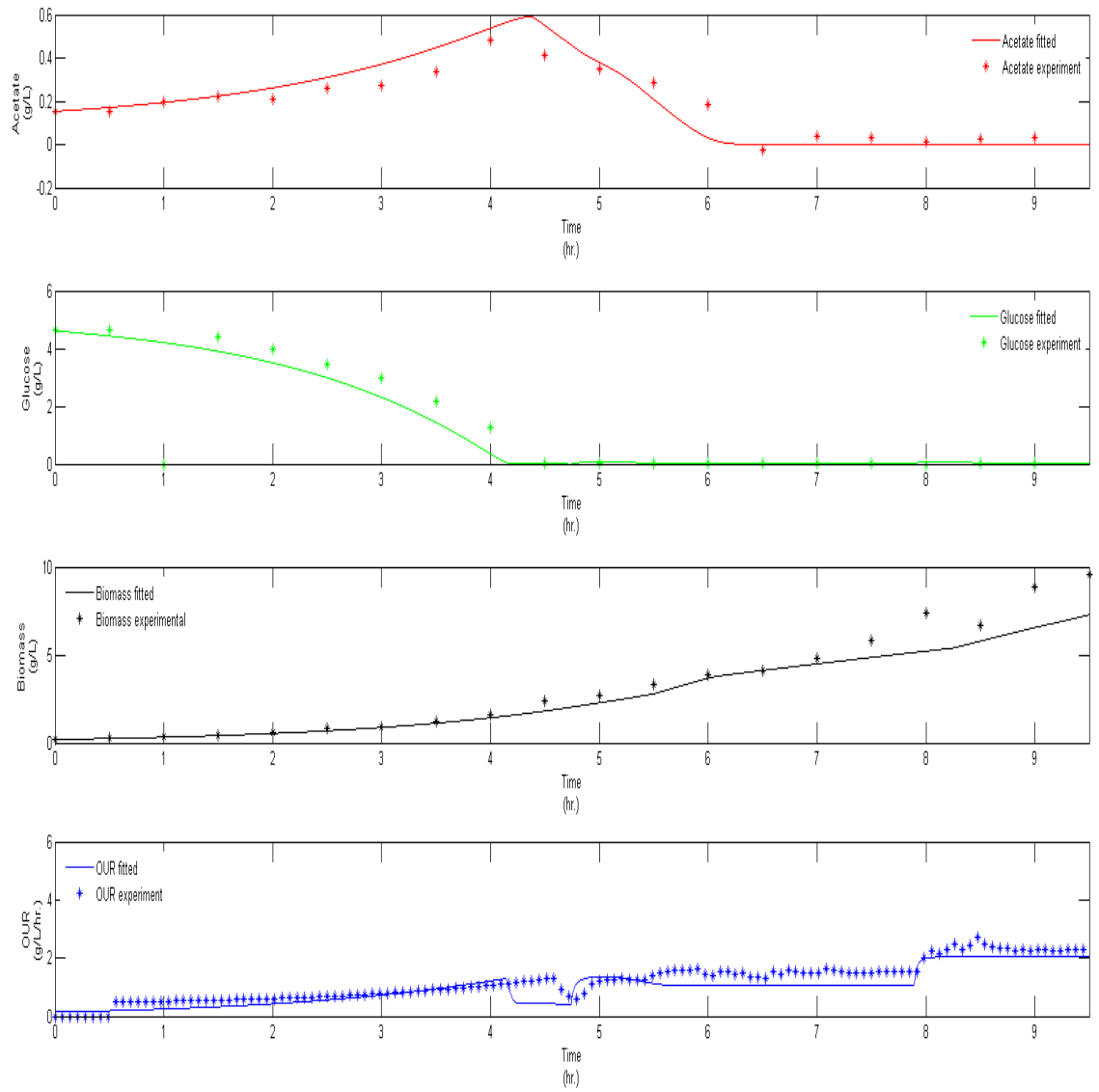


Figure 5.3: Training experiment 3 plots for A , S , X and OUR using fitted parameters.

Variable (units)	Xu Value	Fitted Value
$K_{i,O}$ (g/L)	4.0000	6.999762102368000
$K_{i,S}$ (g/L)	5.0000	8.689703450900000
$qA_{C_{max}}$ (g/Lhr.)	0.2000	0.236917644789370
q_m (g/Lhr.)	0.0400	0.069879903886394
qO_{max} (g/Lhr.)	0.4290	0.750040424418578
qS_{max} (g/Lhr.)	1.2500	1.592771481184673
$Y_{X/A}$ (g/g)	0.4100	0.090888556829738
$Y_{X/S_{of}}$ (g/g)	0.1510	0.270537251296590
$Y_{X/S_{ox}}$ (g/g)	0.5110	0.401978605025204

Table 5.2: Growth block parameter numerical minimization best fit values.

5.2 Fitting Limitations

The fitted parameter results depend on many factors. The most important factor that affects the fitting results is the number of offline sample points available to fit against. The frequency of sampling for the first training experiment is once every hour, and the sampling rate for the other two training experiments is every half an hour. This directly affects the fitting results. The OUR data is available at 5 second intervals which is the sample time set in the BlueSens OPC server for logging frequency. This is an online measurement. The individual curves need to be weighed according to the sample frequency and the magnitude of change observed between data points. Another limitation is with the measurement of acetate and glucose concentration levels from the offline samples. As discussed in Section 4.0.3, the sampled biomaterial is spun down and the solid biomaterial is discarded and the remaining solution is frozen for analysis. In the case of glucose a YSI 2900 meter is used to measure concentration. Depending on the type of membrane used in the YSI, corresponding levels of accuracy can be seen in the offline glucose concentration measurements. The YSI membrane available in the lab has a precision of 0.02(g/L)

with an accuracy of $\pm 2\%$. In the case of acetate concentration measurements, an acetate assay kit is used. Kit A0504–85 by BioAssay is the acetate assay kit available in the lab. The acetate assay kit uses enzyme-coupled reactions to form colored, fluorescent product. The detection range of this kit is $0.20 - 20mM$ acetate for colorimetric assays and $0.13 - 2.0mM$ for fluorimetric assays. The colorimetric assay measures the change in light absorption while the fluorimetric assay uses difference in fluorescence of substrate. For the simulation to switch from overflow metabolism to oxidative metabolism at the end of batch phase, it is essential that zero acetate concentration levels are detected in the fermentation. The accuracy of measurement can affect this condition and can result in the simulation remaining in overflow longer than it should be.

5.3 Result Analysis

The verification dataset is fitted with the minimization parameters and the results can be seen in Figure 5.4. The same experiment is plotted for, using the Xu parameters for comparison Figure 5.5.

To compare the performance of the simulation while using the fitted parameters versus the Xu parameters, the errors associated with each of the four terms of the objective function can be compared as seen in Table 5.3. The root mean square errors of each of the curves in the objective expression for the verification experiment is also shown in Table 5.3.

Parameters Used	Acetate Error	Glucose Error	Biomass Error	OUR Error
Xu Parameters	4.87	6.68	20.15	8.74
Fitted Parameters	2.35	3.55	12.85	5.88

Table 5.3: Error comparison for Fitted vs Xu parameters for the verification experiment.

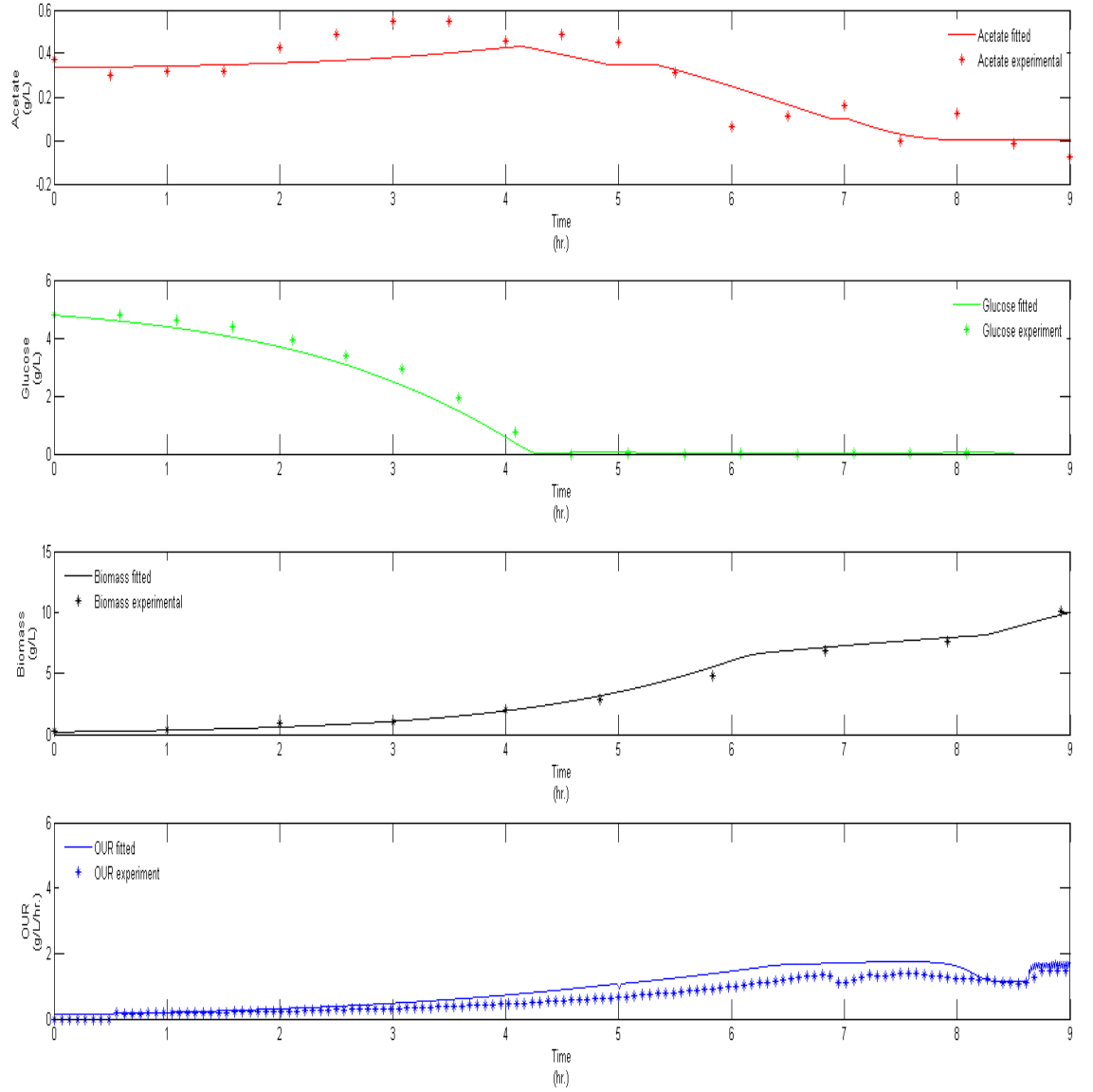


Figure 5.4: Verification experiment plots for A , S , X and OUR using fitted parameters.

The RMS errors are calculated as the root mean square error values between the experimentally logged data points and the simulated value at those time steps

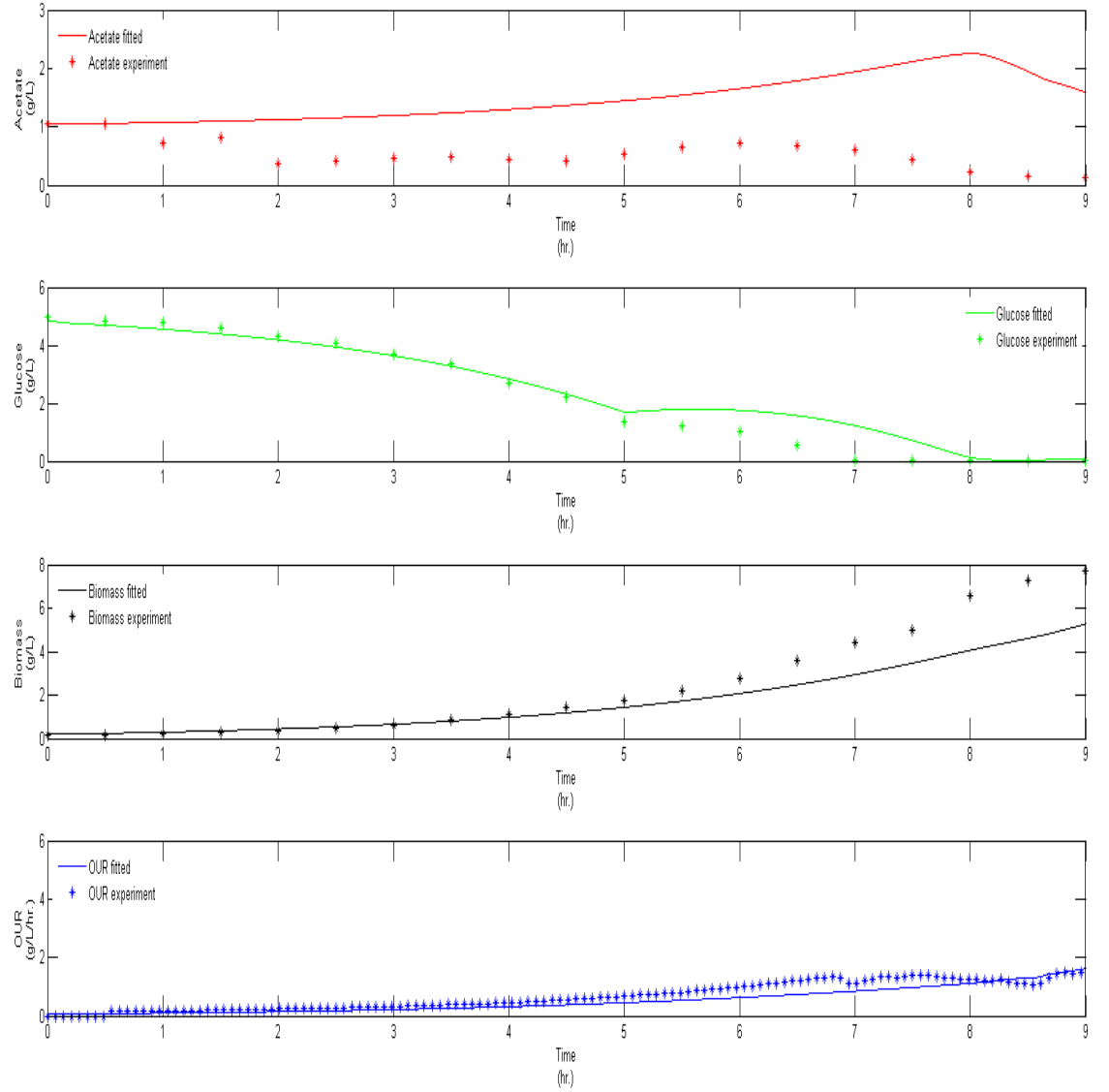


Figure 5.5: Verification experiment plots for A , S , X and OUR using Xu parameters.

for each of the curves used in the objective function expression, A , S , X and OUR . The RMS errors for the fitter parameters are computed for the verification experiment and compared to the original Xu parameters [2] for the same verification experiment.

This gives a clear metric to compare the performance between the fitted parameters and the original Xu parameters.

The errors in Table 5.3 do not include the weight terms specified in Table 5.4. For this minimization, the weights associated with each term are shown in Table 5.4.

Fitting Term	Weight
Acetate Concentration	1500
Glucose Concentration	20
Biomass Concentration	20
OUR	1

Table 5.4: Objective function weights for each term.

The reason for large Biomass error is that the value of X is exponentially increasing with increasing culture time and so, to accurately account for all terms in Equation 5.2, the terms are given their respective error weights. *OUR* error values are also large because of the number of sample points available to fit to. This is because the off-gas sensor used to record *OUR* data is an online sensor that records data every 5 seconds, throughout the fermentation process as compared to offline measurements A , S and X which are recorded only every half an hour in the case of the verification experiment used in this thesis. The acetate weight is the highest as for most of the batch phase, there is acetate present in the system but the fed batch typically is started when most of the acetate is consumed during the metabolite consumption phase. Therefore, it is of critical importance to accurately fit to this drop in the acetate level as the simulation will exit overflow only when the acetate level in the system is zero. There is significant emphasis given to fitting biomass correctly, as the simulation needs to be able to accurately fit biomass for it to be a viable means to test control strategies. As discussed in Section 1.1. The original Xu model has

trouble fitting acetate concentration A . The fitted parameters in comparison perform significantly better. This, along with the addition of OUR as a sensor for which data can be logged online and fitted to, makes the simulation model more precise as there are more data points to fit to. OUR is also a good indicator of metabolic activity, in combination with A , S and X .

Chapter 6

Conclusion and Future Work

The design and implementation of simulation platforms for modeling and parameter estimation of *E. coli* metabolism is presented in this thesis. The process of numerical minimization is also described. The combination of these two simulation models allows for a combined setup that can effectively allow for dynamic parameter estimation and control strategy testing.

6.0.1 Conclusion

The FermCtrl model is used for hardware-in-the-loop implementation of the physical hardware system that communicates with the simulation using Matlab's OPC toolbox. It is possible to log data from the OPC server as well as write values to the various sensors controlled by the DCU. This is able to run in-tandem with the FermSim model which is a simulated model that is used to replicate the behavior of the physical hardware setup. The combination of these systems offers a complete platform to test and configure fermentation control protocols and verify results in an accurate and fast manner effectively. The FermCtrl model is able to interact with the DCU with the use of OPC read/write blocks and the system can be used to effectively

take over all control of sensors from the DCU and allows control to be handed over to a remote system with the help of simulink.

The FermSim model is able to reliably display expected bioprocess behavior extremely quickly. A typical fermentation run that can take 12-20 hours is simulated in a matter of seconds and with the implementation of parameter fitting, it is possible to accurately observe trends and implement control strategies. The combination of the FermSim model for development and the FermCtrl model for testing makes this a very useful system. With many different strains of *E. coli* being developed, it is important to tune the simulation system to the behavior of that strain. With the Xu model, data sets from only a few experiments can fit pre- and post-induction behavior for a strain. This is made possible using the numerical minimization algorithm, in conjunction with the FermSim model. *E. coli* strains with the different plasmids and even the same strains with different amounts of IPTG can have drastically different behavior [8, 28]. Once the strain has been characterized, work can begin on different estimator and control designs. The FermSim model is able to compare different test control strategies as well as equate them to published algorithms. By conventional means, it is hard to compare algorithms implemented using different strains and with different experimental conditions. The development of the described model makes this easy to implement.

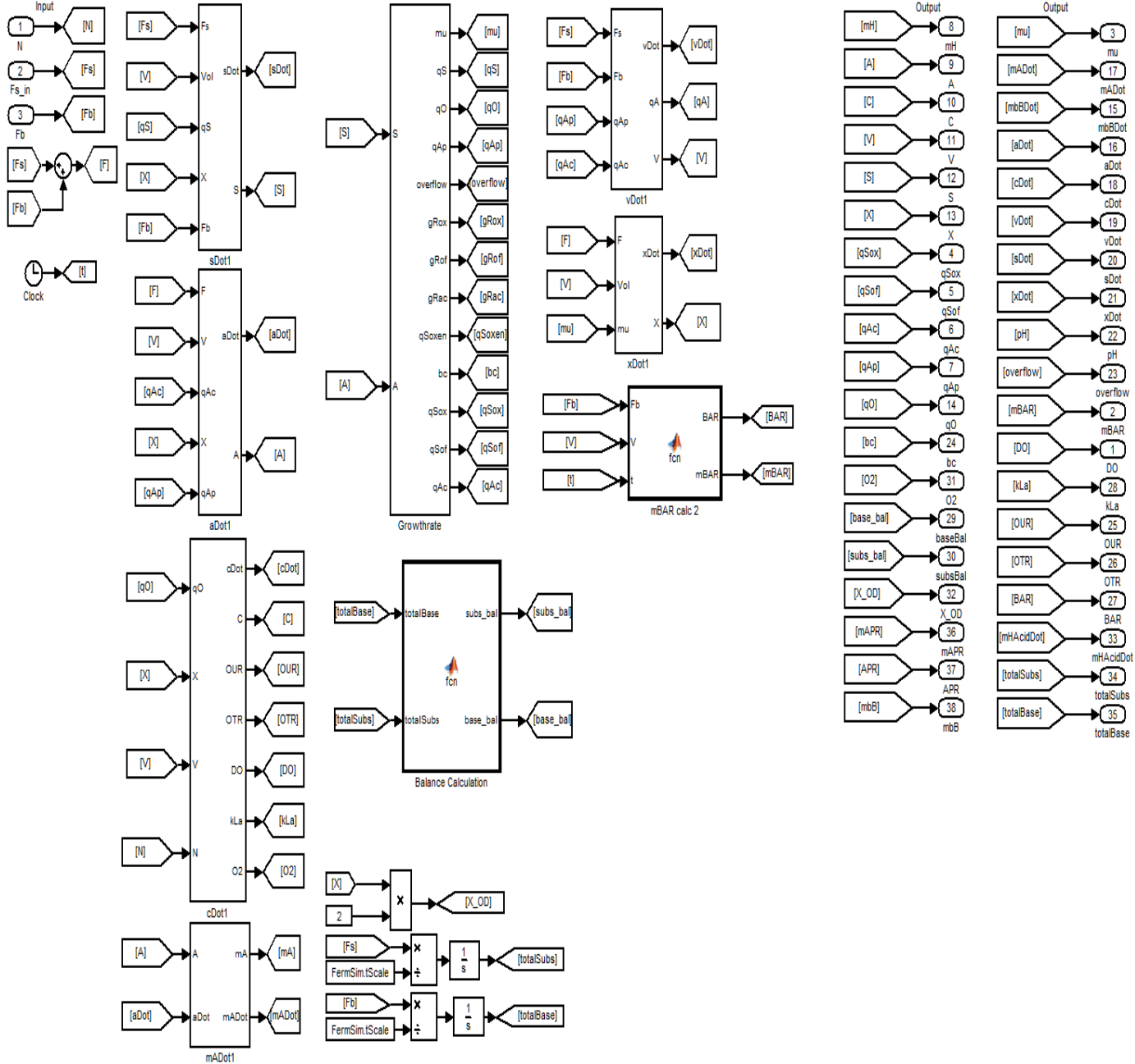
6.0.2 Future Work

It is possible to use the same overall structure and add additional estimators to improve simulation behavior and more effectively capture metabolic activity. This can lead to additional terms in the objective function which can improve the fitting of parameters further. Different fermentation experiments can be simulated by

making the necessary changes to the bioreactor block. FermSim has been developed in a multi-level format that allows simplified swapping in and out of required blocks with a variable tagging architecture. This means that the required variables or constant parameters need to be altered in only one location in the model and the updated version is carried to all levels of the simulated model including all sub-blocks by the means of reference tags. This makes it very convenient to make changes and test various fitting strategies and control methods. Additionally, this will also allow similar parameter estimation and control strategy testing to be run for various other bioprocesses as only the relevant tags need to be altered accordingly.

Appendices

Appendix A FermSim Model



rameters used to simulate culture metabolism. The matlab workspace contains information of all the initial values which are experiment specific. A full list of variables in the initialization file can be seen in Table 1. A typical sub-module is shown in Figure 3.

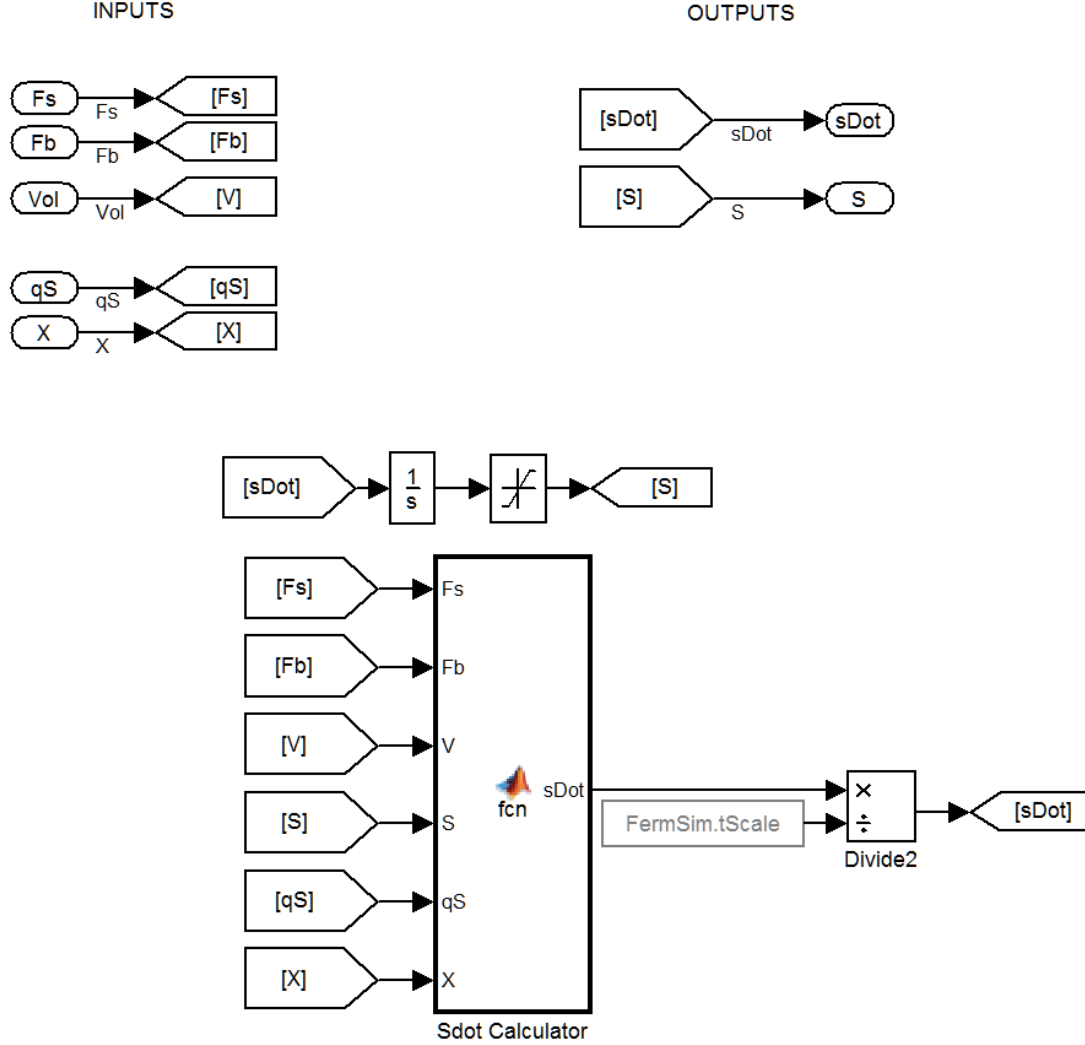


Figure 3: The S sub-module block.

The initial values are stored in a .mat file, FermSim.mat. This file also includes a list of parameters that is currently being used by the growth rate block in the

FermSim model.

Variable Name (units)	Description
expDur (hr.)	Duration of experiment
fbStart (hr.)	Fed-batch start time
tScale (sec/hr.)	Sec-to-hour conversion
Cstar (%)	DO conc. in equilibrium
C (%)	Current DO level
N0 (rpm)	Initial stir speed of motor shaft
V0 (L)	Initial volume
A0 (g/L)	Initial acetate conc.
S0 (g/L)	Initial glucose conc.
X0 (g/L)	Initial biomass conc.
PHset	pH set point
buffer (mM)	Buffer molarity
Mass _s ubs(<i>g</i>)	Initial glucose balance reading
Mass _b ase(<i>g</i>)	Initial base balance reading
Xu	Struct of all Xu parameters

Table 1: List of sensors and communication protocols used.

Appendix B Experiment Details

A single database with all offline and online variables was created for ease of use during simulation and parameter minimization. The complete list of variables associated are shown in Table 2. A total of ten experiments were performed with *E. coli* and data for all ten experiments is available in the experiment database.

Variable (units)	Description
expi.toff (hr.)	offline data time step
expi.Acetate (g/L)	offline acetate measurement
expi.Glucose (g/L)	offline glucose measurement
expi.OD	offline optical density measurement
expi.ton (s)	online data time step
expi.Data(:,1) (%)	substrate set point
expi.Data(:,2) (%)	substrate value
expi.Data(:,3) (rpm)	stir speed set point
expi.Data(:,4) (rpm)	stir speed value
expi.Data(:,5) (L/min)	pump set point
expi.Data(:,6) (L/min)	pump value
expi.Data(:,7) ($^{\circ}C$)	temperature set point
expi.Data(:,8) ($^{\circ}C$)	temperature value
expi.Data(:,9) (%)	DO set point
expi.Data(:,10) (%)	DO value
expi.Data(:,11)	pH set point
expi.Data(:,12)	ph value
expi.Data(:,13) (L/min)	Mass flow rate set point
expi.Data(:,14) (L/min)	Mass flow rate value
expi.Data(:,15) (g)	Balance A value
expi.Data(:,16) (g)	Balance B value
expi.Data(:,17) (%)	Off-gas oxygen value
expi.Data(:,18)	Off-gas rel. humidity
expi.Data(:,19) ($^{\circ}C$)	Off-gas temperature
expi.Data(:,20) (bar)	Off-gas pressure
expi.Data(:,21) (g)	Base totalizer value
expi.Data(:,22) (%)	Off-gas CO_2 value
expi.Data(:,23)	Pseudo real-time violation
expi.Data(:,24) (%)	Gasmx set point
expi.Data(:,25) (%)	Gasmx value

Table 2: List of all online and offline variables recorded in database. Experiment number is denoted by i .

Bibliography

- [1] R. Jayaraj and P. Smooker, “So you need a protein - a guide to the production of recombinant proteins,” *Open Veterinary Science Journal*, vol. 3, pp. 28–34, 2009. [Online]. Available: <http://www.bentham-open.org/pages/gen.php?file=28TOVSJ.pdf&PHPSESSID=f5293cfc476d572c6840b8e34701e4a>
- [2] B. Xu, M. Jahic, and S. O. Enfors, “Modeling of overflow metabolism in batch and fed-batch cultures of escherichia coli,” *Biotechnology progress*, vol. 15, no. 1, pp. 81–90, Jan-Feb 1999.
- [3] L. Wang, Master’s thesis, Clemson University, 2014.
- [4] Y. Pomerleau and M. Perrier, “Estimation of multiple specific growth rates in bioprocesses,” *AIChE Journal*, vol. 36, no. 2, pp. 207–215, 1990.
- [5] A. Rodriguez, G. Quiroz, J. D. Leon, and R. Femat, “State and parameter estimation of an anaerobic digester model,” in *Automation Science and Engineering (CASE), 2011 IEEE Conference on*, 2011, pp. 690–695.
- [6] C. Diaz, P. Dieu, C. Feuillerat, P. Lelong, and M. Salome, “Adaptive predictive control of dissolved oxygen concentration in a laboratory-scale bioreactor,” *Journal of Biotechnology*, vol. 43, no. 1, pp. 21–32, Nov 21 1995.
- [7] D. Levisauskas, R. Simutis, D. Borvitz, and A. Lbbert, “Automatic control of the specific growth rate in fed-batch cultivation processes based on an exhaust gas analysis,” *Bioprocess Engineering*, vol. 15, no. 3, pp. 145–150, Aug 1 1996. [Online]. Available: <http://dx.doi.org/10.1007/BF00369618>
- [8] M. Akesson, P. Hagander, and J. P. Axelsson, “A probing feeding strategy for escherichia coli cultures,” *Biotechnology Techniques*, vol. 13, no. 8, pp. 523–528, Aug 1 1999.
- [9] L. V., “On-line estimation of biomass concentration and non stationary parameters for aerobic bioprocesses,” *Journal of Biotechnology*, vol. 46, no. 3, pp. 197–207, 1996. [Online]. Available: <http://www.ingentaconnect.com/content/els/01681656/1996/00000046/00000003/art00197>

- [10] M. Akesson, P. Hagander, and J. P. Axelsson, "A pulse technique for control of fed-batch fermentations," in *Control Applications, 1997., Proceedings of the 1997 IEEE International Conference on*, 1997, pp. 139–144.
- [11] ———, "Avoiding acetate accumulation in escherichia coli cultures using feedback control of glucose feeding," *Biotechnology and bioengineering*, vol. 73, no. 3, pp. 223–230, May 5 2001.
- [12] A. Vicente, J. I. Castrillo, J. A. Teixeira, and U. Ugalde, "On-line estimation of biomass through ph control analysis in aerobic yeast fermentation systems," *Biotechnology and bioengineering*, vol. 58, no. 4, pp. 445–450, 1998.
- [13] H. Valdes-Gonzalez and J. M. Flaus, "State estimation in a bioprocess described by a hybrid model," in *Intelligent Control, 2001. (ISIC '01). Proceedings of the 2001 IEEE International Symposium on*, 2001, pp. 132–137.
- [14] H. Sang, F. Wang, D. He, Y. Chang, and D. Zhang, "On-line estimation of biomass concentration and specific growth rate in the fermentation process," in *Intelligent Control and Automation, 2006. WCICA 2006. The Sixth World Congress on*, vol. 1, 2006, pp. 4644–4648.
- [15] S. Tatiraju, M. Soroush, and R. Mutharasan, "Multi-rate nonlinear state and parameter estimation in a bioreactor," in *American Control Conference, 1998. Proceedings of the 1998*, vol. 4, 1998, pp. 2324–2328 vol.4.
- [16] D. Tingey, K. Busawon, and M. Saif, "Biomass concentration estimation using the extended jordan observable form," in *Control Applications, 2005. CCA 2005. Proceedings of 2005 IEEE Conference on*, 2005, pp. 143–147.
- [17] M. Keulers, "Structure and parameter identification of a batch fermentation process using non-linear modelling," in *American Control Conference, 1993*, 1993, pp. 2261–2265.
- [18] V. Ljubenova and M. Ignatova, "An approach for parameter estimation of biotechnological processes," *Bioprocess Engineering*, vol. 11, no. 3, pp. 107–113, Aug 1 1994. [Online]. Available: <http://dx.doi.org/10.1007/BF00369606>
- [19] V. N. Lubenova, "Stable adaptive algorithm for simultaneous estimation of time-varying parameters and state variables in aerobic bioprocesses," *Bioprocess Engineering*, vol. 21, no. 3, pp. 219–226, Sep 1 1999. [Online]. Available: <http://dx.doi.org/10.1007/s004490050667>
- [20] M. Perrier, S. F. de Azevedo, E. C. Ferreira, and D. Dochain, "Tuning of observer-based estimators: theory and application to the on-line estimation of kinetic parameters," *Control Engineering Practice*, vol. 8, no. 4, pp. 377–388, Apr 2000.

- [21] G. Bastin and D. Dochain, *On-line Estimation and Adaptive Control of Bioreactors*. Amsterdam, Netherlands: Elsevier Science, 1990.
- [22] A. Johnson and S. Goody, “The original michaelis constant: Translation of the 1913 michaelis-menten paper,” *American Chemical Society*, vol. 50, no. 39, p. 82648269, 09 2011.
- [23] A. J. Wolfe, “The acetate switch,” *Microbiology and Molecular Biology Reviews*, vol. 69, no. 1, pp. 12–50, Mar 2005. [Online]. Available: <http://dx.doi.org/10.1128/MMBR.69.1.12-50.2005>
- [24] V. Lubenova, I. Rocha, and E. C. Ferreira, “Estimation of multiple biomass growth rates and biomass concentration in a class of bioprocesses,” *Bioprocess and Biosystems Engineering*, vol. 25, no. 6, pp. 395–406, July 1 2003. [Online]. Available: <http://dx.doi.org/10.1007/s00449-003-0325-1>
- [25] C. Karakuzu, M. Turker, and S. Ozturk, “Modelling, on-line state estimation and fuzzy control of production scale fed-batch baker’s yeast fermentation,” *Control Engineering Practice*, vol. 14, no. 8, pp. 959–974, Aug 2006.
- [26] M. Pepper, “Designing a minimal-knowledge controller to achieve maximum stable growth for an escherichia coli bioprocess,” Ph.D. dissertation, Clemson University, June 2013.
- [27] G. L. Kleman, K. M. Horken, F. R. Tabita, and W. R. Strohl, 1996.
- [28] R. G. Harrison, P. Todd, S. Rudge, and D. P. Petrides, *Bioseparations Science and Engineering*. New York, New York: Oxford University Press, Inc., 2003.